Chapter 8

Invariant Imbedding Methods: Solving the RTE

We are now well prepared to attack the radiance transfer equation (RTE) and its associated boundary conditions. Our attack comes in two steps. First, we must discretize the directionally continuous RTE (5.24) in order to obtain a finite number of equations in the same number of unknowns. This directional discretization will be accomplished using the quad-averaging formalism developed in Chapter 4. Second, we shall solve the resulting discretized equations using the invariant imbedding methods developed in Chapter 7. These two steps in the overall solution process are independent. Quad-averaging is one of several ways to discretize the direction variable $\hat{\xi}$ = (μ, ϕ); we shall encounter another way in Section 9.1. Invariant imbedding is one of many ways to solve the resulting equations. We already have discussed two applicable methods, Monte Carlo and invariant imbedding, and we shall discuss other methods in the next chapter.

We shall find that the directionally discretized version of the RTE leads to equations that have almost exactly the same matrix form as the matrix version (7.37) of the two-flow equations. There are two primary differences in these matrix equations. First, the 1×2 matrix $\underline{E}(z) = [E_u(z), E_d(z)]$ seen in the two-flow equations will be replaced by a $1 \times N$ matrix containing certain Fourier amplitudes, from which the radiance distribution can be easily obtained. Second, the 2×2 local transfer matrix $\underline{K}(z)$ will become an $N \times N$ matrix *determined solely by the inherent optical properties of the water body*. Once the radiance-amplitude matrix equation has been obtained, all of the solution formalism developed for the two-flow equations will become applicable to the solution of the RTE.

Most of our effort in this chapter is devoted to the steps leading from the RTE, Eq. (5.24), to the radiance-amplitude equation, Eq. (8.59). This transformation is rather tedious, but it is crucial to the development of an efficient numerical algorithm for solving the RTE in a mathematical setting that mimics the physical setting of natural waters. Similar transformations are also used in developing other numerical methods, such as the discrete-

ordinates method to be described in Section 9.1. Therefore, familiarity with the process pays dividends beyond our immediate needs. We shall resist the temptation to gloss over the messy parts via the incantation "it can be shown." Nevertheless, whenever possible, we shall omit the mathematical details of our derivations; these may be found to the last subscript in Mobley and Preisendorfer (1988).

In this chapter we again encounter "barred" headings, which denote material dealing with numerical details. These sections can be skipped by readers interested only in a general overview of the solution method.

8.1 The RTE as a Mathematics Problem

Table 7.1 displays the two-flow equations and their boundary conditions. Table 8.1 displays a corresponding summary of the radiance-level equations. Equations (8.1) and (8.2) are just Eqs. (4.3) and (4.4), which describe the boundary conditions to be satisfied at the air-water surface $S[a,w]$. The physical interpretation of these equations was discussed in detail in Section 4.1. Quad-averaged, i.e. directionally discretized, versions of these boundary equations were developed in Section 4.7; recall Eqs. (4.66) and (4.67). The quad-averaged versions of the four bi-directional surface reflectance and transmittance functions were numerically evaluated and discussed in Section 4.8. We therefore consider the surface r and t functions (or at least their quad-averaged forms) to be known. We also assume that the air-incident radiance distribution $L(a;\hat{\xi})$, $\hat{\xi} \in \Xi_d$, is known.

Equation (8.3) is just the RTE (5.24). We shall work with the RTE as a function of optical depth ζ, and we omit the wavelength argument for brevity. For notational simplicity, we write the source term in Eq. (5.24) as

$$\tilde{S}(\zeta;\hat{\xi}) \equiv \frac{1}{c(\zeta)} S(\zeta;\hat{\xi}) .$$

As always, we assume that the IOP's of the water body are given. Thus ω_o, $\tilde{\beta}$, $\tilde{S}$ and, implicitly, c are considered known.

Equation (8.4) gives the bottom boundary condition for an opaque, reflecting bottom boundary layer $S[m,b]$. This boundary condition specifies the bi-directional radiance reflectance of the medium $S[m,b]$ below optical depth m, the maximum depth at which the radiance distribution is desired. Depth m may be the depth of a physical bottom ($m = b$), or a finite depth in an infinitely deep water body ($b \rightarrow \infty$), below which the IOP's are taken as constant with depth. Equation (4.81) gives $r(m,b;\hat{\xi}' \rightarrow \hat{\xi})$ for a

Table 8.1. The time-independent, one-dimensional radiance transfer equation and associated boundary conditions. The underlined quantities are assumed known. Compare with Tables 7.1 and 8.2.

water layer	equations to be satisfied	equation number
$S[a,w]$	$L(a;\xi) = \int_{\Xi_u} L(w;\xi') \, \underline{t(w,a;\xi' \to \xi)} \, d\Omega(\xi') + \int_{\Xi_d} \underline{L(a;\xi')} \, \underline{r(a,w;\xi' \to \xi)} \, d\Omega(\xi')$ for $\xi \in \Xi_u$	(8.1)
	$L(w;\xi) = \int_{\Xi_u} L(w;\xi') \, \underline{r(w,a;\xi' \to \xi)} \, d\Omega(\xi') + \int_{\Xi_d} \underline{L(a;\xi')} \, \underline{t(a,w;\xi' \to \xi)} \, d\Omega(\xi')$ for $\xi \in \Xi_d$	(8.2)
$S[w,m]$	$\mu \dfrac{dL(\zeta;\xi)}{d\zeta} = -L(\zeta;\xi) + \underline{\omega_o(\zeta)} \int_{\Xi} L(\zeta;\xi') \, \underline{\tilde{\beta}(\zeta;\xi' \to \xi)} \, d\Omega(\xi') + \underline{\tilde{S}(\zeta;\xi)}$ for $\xi \in \Xi$	(8.3)
$S[m,b]$	$L(m;\xi) = \int_{\Xi_d} L(m;\xi') \, \underline{r(m,b;\xi' \to \xi)} \, d\Omega(\xi')$ for $\xi \in \Xi_u$	(8.4)

Lambertian reflecting bottom. We shall learn in Chapter 9 how to evaluate $r(m,b;\hat{\xi}'\to\hat{\xi})$ for an infinitely deep water body. In either case, the bottom reflectance is known. These two cases – a finite-depth, Lambertian bottom or infinitely deep, homogeneous water – take care of most situations of oceanographic and limnologic relevance. The extension of the solution procedure to the case of a completely general, transmitting bottom boundary with external radiance incident upward on the lower side of the bottom boundary easily can be made by readers wishing to model glass-bottomed aquariums.

We also exclude the possibility of internal sources within the boundaries $S[a,w]$ and $S[m,b]$ themselves. This is reasonable for oceanographic problems, in which $S[a,w]$ is the air-water surface and depth m can be chosen below the depth of any significant bioluminescence or fluorescence. We do allow for internal sources within the water body $S[w,m]$.

It is now easy to state our problem: *Solve Eqs. (8.1)-(8.4) for the radiance distribution* within the water body, $L(\zeta;\hat{\xi})$, $\hat{\xi} \in \Xi$, $w \leq \zeta \leq m$, *and for the water-leaving radiance*, $L(a,\hat{\xi})$, $\hat{\xi} \in \Xi_u$. The solution proceeds as follows.

8.2 Quad Averaging the RTE ▐▌

In Section 4.7 we discussed the necessity of directionally discretizing the radiance and the boundary reflectance and transmittance functions. To achieve this discretization, we first partitioned the unit sphere Ξ into a finite number of *quads,* which are bounded by lines of constant θ (or μ) and ϕ. We then introduced quad-averaging operators for functions of a single direction, Eq. (4.52), and for bi-directional functions, Eq. (4.63). Applying these operators to the boundary conditions (8.1) and (8.2) led to the quad-averaged boundary conditions seen in Eqs. (4.66) and (4.67).

The same quad-averaging process must be applied to the RTE itself. This is easily done. For example, left hand side of Eq. (8.3) becomes

$$\frac{1}{\Omega_{uv}} \int_{\xi \in Q_{uv}} \left\{ \mu \, \frac{dL(\zeta;\hat{\xi})}{d\zeta} \right\} d\Omega(\hat{\xi}) \tag{8.5a}$$

$$= \frac{1}{\Omega_{uv}} \int_{\mu_u(1)}^{\mu_u(2)} d\mu \int_{\phi_v(1)}^{\phi_v(2)} d\phi \left\{ \mu \, \frac{d}{d\zeta} \left[\sum_p \sum_q \chi_{pq}(\mu,\phi) \, L(\zeta;p,q) \right] \right\} \tag{8.5b}$$

$$= \sum_p \sum_q \left[\frac{d}{d\zeta} L(\zeta;p,q) \right] \frac{1}{\Omega_{uv}} \int_{\mu_u(1)}^{\mu_u(2)} d\mu \int_{\phi_v(1)}^{\phi_v(2)} d\phi \ \mu \ \chi_{pq}(\mu,\phi) \qquad (8.5c)$$

$$= \sum_p \sum_q \left[\frac{d}{d\zeta} L(\zeta;p,q) \right] \frac{1}{\Omega_{uv}} \delta_{p-u} \delta_{q-v} \int_{\mu_u(1)}^{\mu_u(2)} \mu \ d\mu \int_{\phi_v(1)}^{\phi_v(2)} d\phi \qquad (8.5d)$$

$$= \left[\frac{d}{d\zeta} L(\zeta;u,v) \right] \frac{1}{\Delta\mu_u \Delta\phi_v} \mu_u \Delta\mu_u \Delta\phi_v = \mu_u \frac{dL(\zeta;u,v)}{d\zeta} . \qquad (8.5e)$$

In going from Eq. (8.5a) to (8.5b), we have formally replaced the directionally continuous $L(\zeta;\hat{\xi})$ by the step-function form shown in Eq. (4.53). Subsequent equations have used the definition of $\chi_{pq}(\mu,\phi)$ given in Eq. (4.54), and the reduction of $\int\int\mu d\mu d\phi$ was done as in Eq. (4.59).

　　The integral term in Eq. (8.3) has exactly the same form as the integrals in the surface boundary conditions. This term is quad-averaged just as in Eqs. (4.63) to (4.66), and the result is

$$\omega_o(\zeta) \sum_r \sum_s L(\zeta;r,s) \ \tilde{\beta}(\zeta;r,s\to u,v) .$$

Here the sum over all quads Q_{rs} is interpreted as shown in Eq. (4.62). The *quad-averaged phase function* has the form of Eq. (4.63), namely

$$\tilde{\beta}(\zeta;r,s\to u,v) = \frac{1}{\Omega_{uv}} \iint_{Q_{uv}} d\mu \ d\phi \iint_{Q_{rs}} d\mu' \ d\phi' \ \tilde{\beta}(\zeta;\mu',\phi'\to\mu,\phi) . \qquad (8.6)$$

　　Collecting the above results gives the *quad-averaged* RTE:

$$\mu_u \frac{d}{d\zeta} L(\zeta;u,v) = -L(\zeta;u,v)$$
$$+ \ \omega_o(\zeta) \sum_r \sum_s L(\zeta;r,s) \ \tilde{\beta}(\zeta;r,s\to u,v) \ + \ \tilde{S}(\zeta;u,v) , \qquad (8.7)$$

which holds for all Q_{uv} in Ξ. *Note that although Eq. (8.7) is a discrete function of direction, it is still a continuous function of depth and wavelength.*

　　Equation (8.7) is to be solved along with the quad-averaged surface boundary conditions (4.66) and (4.67), and with the similar quad-averaged version of the lower boundary condition (8.4). These equations are collected for reference in Table 8.2. The quad-averaged Eqs. (8.8)-(8.11) give us a finite number of equations to be solved for the finite number of quad-

Table 8.2. The quad-averaged versions of Eqs. (8.1)-(8.4). The underlined quantities are assumed known.

water layer	equations to be satisfied	equation number
$S[a,w]$	$L(a;u,v) = \sum_r \sum_s \limits_{Q_{rs} \in \Xi_u} L(w;r,s)\, \underline{t(w,a;r,s \to u,v)}$ $\qquad\qquad + \sum_r \sum_s \limits_{Q_{rs} \in \Xi_d} \underline{L(a;r,s)}\, \underline{r(a,w;r,s \to u,v)} \qquad$ for $Q_{uv} \in \Xi_u$	(8.8)
	$L(w;u,v) = \sum_r \sum_s \limits_{Q_{rs} \in \Xi_u} L(w;r,s)\, \underline{r(w,a;r,s \to u,v)}$ $\qquad\qquad + \sum_r \sum_s \limits_{Q_{rs} \in \Xi_d} \underline{L(a;r,s)}\, \underline{t(a,w;r,s \to u,v)} \qquad$ for $Q_{uv} \in \Xi_d$	(8.9)
$S[w,m]$	$\mu_u \dfrac{dL(\zeta;u,v)}{d\zeta} = -L(\zeta;u,v) + \underline{\omega_o(\zeta)} \sum_r \sum_s \limits_{Q_{rs} \in \Xi} L(\zeta;r,s)\, \underline{\tilde{\beta}(\zeta;r,s \to u,v)} + \underline{\tilde{S}(\zeta;u,v)} \qquad$ for $Q_{uv} \in \Xi$	(8.10)
$S[m,b]$	$L(m;u,v) = \sum_r \sum_s \limits_{Q_{rs} \in \Xi_d} L(m;r,s)\, \underline{r(m,b;r,s \to u,v)} \qquad$ for $Q_{uv} \in \Xi_u$	(8.11)

averaged radiances. If the unit sphere Ξ has been partitioned into N quads, then Eq. (8.10) generates a set of N coupled, ordinary differential equations. These equations are to be solved as a two-point boundary value problem subject to the quad-averaged boundary conditions (8.8), (8.9) and (8.11). The parallel with the two-flow problem of Section 7.1 is becoming apparent.

In Section 4.8 we saw how to estimate the quad-averaged surface reflectance and transmittance functions by numerical simulation of random water surfaces and Monte Carlo ray tracing. Problem 8.1 shows how to evaluate $r(m,b;r,s{\rightarrow}u,v)$ for a Lambertian bottom boundary, and Section 9.5 shows how to compute this quantity for an infinitely deep, homogeneous layer of water $S[m,\infty]$. The quad-averaged source function $\tilde{S}(\zeta;u,v)$ can be computed by performing the integration (numerically if necessary) shown in Eq. (4.52), once the source function $\tilde{S}(\zeta;\theta,\phi)$ is specified along with the other IOP's. We next discuss how to compute the quad-averaged phase function.

Numerical evaluation of the quad-averaged phase function ▌▌

The quad-averaged phase function $\tilde{\beta}(\zeta;r,s{\rightarrow}u,v)$ can be determined by evaluating the quadruple integral shown in Eq. (8.6). The computational expense of evaluating this integral could be prohibitive if we had to recompute $\tilde{\beta}(\zeta;r,s{\rightarrow}u,v)$ at many depths as we solved the RTE. We therefore model the total phase function as a sum of component phase functions, as was done in Eq. (3.13):

$$\tilde{\beta}(\zeta;r,s{\rightarrow}u,v) = \sum_{i=1}^{N_s} \frac{b_i(\zeta)}{b(\zeta)} \tilde{\beta}_i(r,s{\rightarrow}u,v) . \qquad (8.12)$$

Here N_s is the number of scattering constituents in the water. Often, $N_s = 2$, with $i = 1$ representing pure sea water and $i = 2$ representing "particles." In this case, $\tilde{\beta}_1$ is obtained by quad averaging the $\tilde{\beta}_w$ of Eq. (3.30), and $\tilde{\beta}_2$ is obtained from the particle phase function $\tilde{\beta}_p$ of Table 3.10. Since we are forcing the depth dependence to reside in the scattering coefficients $b_i(\zeta)$, *we need to evaluate Eq. (8.6) only once for a given phase function.* The depth dependence of the total phase function is then obtained from the $b_i(\zeta)/b(\zeta)$ factors in Eq. (8.12).

For constituent phase functions $\tilde{\beta}_i(\mu',\phi'{\rightarrow}\mu,\phi) \equiv \tilde{\beta}_i(\psi)$ that are highly peaked in the forward-scattering direction, the integrations in Eq. (8.6) must be performed numerically and with great care. Fortunately, the phase-function symmetries seen in Eq. (5.7) mean that it is not necessary to integrate Eq. (8.6) for all possible pairs of quads Q_{rs} and Q_{uv}. Indeed, we

can set $s = 1$ (the quads centered on $\phi' = 0$) and vary v from 1 to $n+1$ (recall the quad numbering scheme of Section 4.7, in which $v = 1, 2,..., 2n$ for $0 \le \phi_v < 2\pi$, with $\phi_{n+1} = \pi$). This is the discrete equivalent of setting $\phi' = 0$ and letting ϕ range from 0 to π in order to generate all possible values of $\cos(\phi - \phi')$.

In order to achieve sufficient resolution of highly peaked phase functions, it is usually necessary to divide the quads into "subquads," at least when Q_{rs} and Q_{uv} are near together, i.e. when the scattering angle ψ is small. Then Eq. (8.6) can be evaluated as (dropping the "constituent" subscript i)

$$\tilde{\beta}(r,1 \to u,v) = \frac{1}{\Omega_{uv}} \sum_{i=1}^{n_\mu} \delta\mu_i \sum_{j=1}^{n_\phi} \delta\phi_j \sum_{k=1}^{n_\mu} \delta\mu_k \sum_{l=1}^{n_\phi} \delta\phi_l \, \tilde{\beta}(\psi_{ijkl}) \,, \qquad (8.13)$$

where the scattering angle is determined from Eq. (1.11):

$$\cos\psi_{ijkl} = \mu_k' \mu_i + \sqrt{1 - \mu_k'^{\,2}} \, \sqrt{1 - \mu_i^2} \, \cos(\phi_l - \phi_j) \,.$$

In Eq. (8.13), n_μ is the number of μ-subquads into which we have divided quad Q_{uv}; $n_\mu \ge 1$. Thus $\delta\mu_i \equiv \Delta\mu_u/n_\mu$, and likewise for n_ϕ and $\delta\phi_j$, etc. Note that even though we have set $s = 1$, we still must integrate ϕ' over the range $\Delta\phi_1'$ of the quad Q_{r1} centered on $\phi' = 0$. If $\tilde{\beta}(\psi)$ is known only at a set of discrete scattering angles, the value of $\tilde{\beta}\tilde{\beta}(\psi_{ijkl})$ can be obtained by interpolation between the known values. Since most "particle-like" $\tilde{\beta}$'s are roughly linear on a $\log\tilde{\beta}$ versus $\log\psi$ plot, linear interpolation in the logarithms usually produces accurate values for $\tilde{\beta}\tilde{\beta}(\psi_{ijkl})$.

The numerically most difficult evaluation of Eq. (8.13) occurs when $(u,v) = (r,1)$, which is the quad-averaged equivalent of forward scattering. Then we must evaluate $\tilde{\beta}$ at very small scattering angles, or even at $\psi = 0$. However, we can avoid the numerical evaluation of the forward-scattering term by use of the normalization condition (3.8),

$$\int_{\hat{\xi} \in \Xi} \tilde{\beta}(\hat{\xi}' \to \hat{\xi}) \, d\Omega(\hat{\xi}) = \int_{-1}^{1} \int_{0}^{2\pi} \tilde{\beta}(\mu',\phi' \to \mu,\phi) \, d\mu \, d\phi = 1,$$

which holds for all $\hat{\xi}' = (\mu',\phi')$ in Ξ. Quad averaging this equation in the usual manner gives

$$\frac{1}{\Omega_{rs}} \sum_u \sum_v \tilde{\beta}(r,s \to u,v) \, \Omega_{uv} = 1 \,,$$

which holds for all Q_{rs} in Ξ. Solving this equation for the forward-scatter

term $(r,s) = (u,v) = (r,1)$ gives

$$\tilde{\beta}(r,1{\rightarrow}r,1) \;=\; 1 \;-\; \frac{1}{\Omega_{r1}} \sum_{u} \sum_{\substack{v \\ (u,v) \neq (r,1)}} \tilde{\beta}(r,1{\rightarrow}u,v).$$

(8.14)

It is numerically efficient to determine all non-forward-scatter values of $\tilde{\beta}(r,s{\rightarrow}u,v)$ using Eq. (8.13), and then to apply Eq. (8.14) to obtain the value for the forward-scatter case. This procedure also minimizes errors arising from inaccurate knowledge of the phase function at very small scattering angles.

An equation corresponding to Eq. (8.6) was first employed by Acquista, *et al.*, (1981). They effected the numerical evaluation of the quadruple integral by first expanding the phase function in Legendre polynomials. As we shall see in Section 9.1, such an expansion is not well suited to the highly peaked phase functions encountered in hydrologic optics. However, they clearly recognized *the main conceptual and numerical advantage of the quad-averaging formalism: its ability to handle arbitrary phase functions*.

Quad averaging the effective source function ▌▌

The mechanism for computing the quad-averaged, effective source function $\tilde{S}(\zeta;u,v)$ seen in Eq. (8.7) follows immediately from its definition. Recall from Eqs. (5.24) and (5.21) that

$$\tilde{S}(\zeta;\mu,\phi) \;\equiv\; \frac{1}{c(\zeta)}\Big[L_*^{\mathrm{I}}(\zeta;\hat{\xi}) \;+\; L_*^{\mathrm{S}}(\zeta;\hat{\xi}) \Big],$$

where L_*^{I} is the inelastic scattering path function and L_*^{S} is the path function due to true internal sources. Equation (5.10) gives L_*^{I}:

$$L_*^{\mathrm{I}}(\zeta;\hat{\xi};\lambda) \;=\; \int\limits_{\hat{\xi}' \in \Xi} \int\limits_{\lambda' \in \Lambda} L(\zeta;\hat{\xi}';\lambda') \, \beta^{\mathrm{I}}(\zeta;\hat{\xi}'{\rightarrow}\hat{\xi};\lambda'{\rightarrow}\lambda) \, d\lambda' \, d\Omega(\hat{\xi}').$$

Replacing β^{I} by $b^{\mathrm{I}}\tilde{\beta}^{\mathrm{I}}$ as in Eq. (5.12) gives

$$L_*^{\mathrm{I}}(\zeta;\hat{\xi};\lambda) \;=\; \int\limits_{\lambda' \in \Lambda} d\lambda' \, b^{\mathrm{I}}(\zeta;\lambda'{\rightarrow}\lambda) \int\limits_{\hat{\xi}' \in \Xi} d\Omega(\hat{\xi}') \, L(\zeta;\hat{\xi}';\lambda') \, \tilde{\beta}^{\mathrm{I}}(\hat{\xi}'{\rightarrow}\hat{\xi}).$$

This equation can be quad averaged in the usual manner (e.g., see page 204) to get

$$L_*^{\mathrm{I}}(\zeta;u,v;\lambda) \;=\; \int\limits_{\lambda' \in \Lambda} d\lambda' \, b^{\mathrm{I}}(\zeta;\lambda'{\rightarrow}\lambda) \sum_{r}\sum_{s} L(\zeta;r,s;\lambda') \, \tilde{\beta}^{\mathrm{I}}(r,s{\rightarrow}u,v).$$

(8.15)

We quad average the directional part of the volume inelastic scattering function just as we do for elastic scattering phase functions. The depth dependence of L_*^I results from the depth dependence of the inelastic scattering coefficient b^I and of the radiance itself.

True-emission sources L_*^S can be represented as in Eq. (5.107):

$$L_*^S(\zeta;\hat{\xi};\lambda) = S_o(\zeta;\lambda)\,\tilde{\beta}^S(\hat{\xi}),$$

where $S_o(\zeta;\lambda)$ is the spectral radiant power emitted per cubic meter of water and $\tilde{\beta}^S(\hat{\xi})$ is the angular emission function for the source. When quad averaged using Eq. (4.52), this equation becomes

$$L_*^S(\zeta;u,v;\lambda) = S_o(\zeta;\lambda)\,\tilde{\beta}^S(u,v). \qquad (8.16)$$

For isotropic emission, as in the case of bioluminescence, we have $\tilde{\beta}^S(\hat{\xi}) = 1/4\pi$ sr^{-1}, and Eq. (8.16) reduces to

$$L_*^S(\zeta;u,v;\lambda) = \frac{1}{4\pi}\,S_o(\zeta;\lambda) \qquad (\text{W m}^{-3}\text{ sr}^{-1}\text{ nm}^{-1}).$$

We therefore compute the quad-averaged source function as

$$\tilde{S}(\zeta;u,v) = \frac{1}{c(\zeta)}\Big[L_*^I(\zeta;u,v) + L_*^S(\zeta;u,v) \Big],$$

where L_*^I and L_*^S are given by Eqs. (8.15) and (8.16), respectively.

We now know how to evaluate all of the underlined quantities seen in Eqs. (8.8)-(8.11). We could proceed with the solution of these equations in their present form. However, the computational and computer storage requirements can be greatly reduced if we first decompose Eqs. (8.8)-(8.11) into Fourier, or spectral, amplitudes.

8.3 Fourier Polynomial Analysis ▐▌

Quad averaging leaves us with two discretized angular variables, μ_u and ϕ_v. The methods of Fourier analysis can be used to convert the associated Eqs. (8.8)-(8.11) into sets of equations that depend on only *one* angular variable, μ_u. This transformation will prove to be numerically advantageous because the resulting forms of the discretized equations can be solved as a sequence of independent "small" problems, rather than as one "large" problem. We shall see in Section 8.4 how this is done.

Our first observation is that because Eqs. (8.8)-(8.11) are directionally *discrete equations*, the usual Fourier analysis formulas for continuous functions require modification. We now collect for reference several formulas, which will be needed in the next section.

Discrete orthogonality relations ▌▌

Recall once again from Eq. (4.61) that the quad partitioning Q_{uv} has the non-polar-cap quads centered at

$$\phi_v \equiv (v-1)\,\Delta\phi\,, \text{ for } v = 1, 2, ..., 2n\,,$$

and that $\Delta\phi = \pi/n$ is the same for each quad. (The polar caps are always a special case.) If k and l are positive integers in the range $0 \le k, l \le n$, then

$$\sum_{v=1}^{2n} \cos(k\phi_v)\cos(l\phi_v) = \begin{cases} 0 \text{ if } k \ne l \\ n \text{ if } k = l \text{ and } l = 1, 2, ..., n-1 \\ 2n \text{ if } k = l \text{ and } l = 0 \text{ or } n\,. \end{cases} \quad (8.17\text{a})$$

Using the Kronecker delta symbol of Eq. (1.19), Eq. (8.17a) can be condensed as

$$\sum_{v=1}^{2n} \cos(k\phi_v)\cos(l\phi_v) = n(\delta_{k+l} + \delta_{k-l} + \delta_{k+l-2n})\,. \quad (8.17\text{b})$$

This equation is the discrete equivalent of

$$\int_0^{2\pi} \cos(k\phi)\cos(l\phi)\,d\phi = \pi(\delta_{k+l} + \delta_{k-l}) = \begin{cases} 0 \text{ if } k \ne l \\ \pi \text{ if } k = l \ne 0 \\ 2\pi \text{ if } k = l = 0\,. \end{cases}$$

Note that Eq. (8.17) is similar to the continuous case, but that the value for $k = l = 0$ or n is peculiar to the discrete formula.

Likewise we have

$$\sum_{v=1}^{2n} \sin(k\phi_v)\sin(l\phi_v) = \begin{cases} 0 \text{ if } k \ne l \\ n \text{ if } k = l \text{ and } l = 1, 2, ..., n-1 \\ 0 \text{ if } k = l \text{ and } l = 0 \text{ or } n\,. \end{cases} \quad (8.18)$$

$$= n(\delta_{k-l} - \delta_{k+l} - \delta_{k+l-2n})\,.$$

We also have

$$\sum_{v=1}^{2n} \cos(k\varphi_v) \sin(l\varphi_v) = 0 \text{ for all } k \text{ and } l. \tag{8.19}$$

After application of trigonometric identities and Eqs. (8.17)-(8.19), we obtain the following needed formulas, which hold for $k, l = 0, ..., n\text{-}1$:

$$\sum_{v=1}^{2n} \cos(k\varphi_v) \cos[l(\varphi_s - \varphi_v)] = n(\delta_{k+l} + \delta_{k-l} + \delta_{k+l-2n}) \cos(l\varphi_s) \tag{8.20a}$$

and

$$\sum_{v=1}^{2n} \sin(k\varphi_v) \cos[l(\varphi_s - \varphi_v)] = n(\delta_{k-l} - \delta_{k+l} - \delta_{k+l-2n}) \sin(l\varphi_s) \tag{8.20b}$$

Fourier polynomial formulas ▌▌

Let $f_v \equiv f(\varphi_v)$ be any *discrete* function of the azimuthal angle φ, i.e. f_v is defined only at the discrete values φ_v. An example of such a function is the quad-averaged radiance $L(\zeta;u,v)$, for ζ and u held constant while $v = 1, 2, ..., 2n$ varies. Then f_v has the *Fourier polynomial representation*

$$f_v = \sum_{l=0}^{n} \left[\hat{f}_1(l) \cos(l\varphi_v) + \hat{f}_2(l) \sin(l\varphi_v) \right], \tag{8.21}$$

for $v = 1, 2, ..., 2n$. The quantities $\hat{f}_1(l)$ and $\hat{f}_2(l)$ are called the *spectral cosine* and *spectral sine amplitude,* respectively. This use of "spectral" has nothing to do with the wavelength of light, as it does in "spectral radiance," for example. This confusing terminology can be blamed on historical precedent. Fourier spectral amplitudes will always be denoted by a caret on the symbol representing the physical quantity. Because $\sin(l\varphi_v) = 0$ if $l = 0$ or $l = n$, $\hat{f}_2(0)$ and $\hat{f}_2(n)$ can be chosen arbitrarily. For bookkeeping purposes, it is convenient to define

$$\hat{f}_2(0) \equiv \hat{f}_2(n) \equiv 0.$$

The cosine amplitudes $\hat{f}_1(l)$ are determined by multiplying Eq. (8.21) by $\cos(k\varphi_v)$, summing over v, and applying the orthogonality relations (8.17) and (8.19). The result is

$$\hat{f}_1(l) = \frac{1}{\epsilon_l} \sum_{v=1}^{2n} f_v \cos(l\varphi_v) \quad \text{for } l = 0, 1, ..., n, \tag{8.22a}$$

where we have defined

$$\epsilon_l \equiv n(1 + \delta_{2l} + \delta_{2l-2n}) = \begin{cases} 2n \text{ if } l = 0 \text{ or } l = n \\ n \text{ if } l = 1, 2, ..., n-1 \,. \end{cases} \quad (8.22b)$$

The sine amplitudes are determined in a similar fashion after multiplying Eq. (8.21) by $\sin(k\phi_v)$ and summing over v. The result is

$$\hat{f}_2(l) = \frac{1}{\gamma_l} \sum_{v=1}^{2n} f_v \sin(l\phi_v) \quad \text{for } l = 1, 2, ..., n-1 \,, \quad (8.23a)$$

where

$$\gamma_l \equiv n(1 - \delta_{2l} - \delta_{2l-2n}) = \begin{cases} 0 \text{ if } l = 0 \text{ or } l = n \\ n \text{ if } l = 1, 2, ..., n-1 \,. \end{cases} \quad (8.23b)$$

Note that the values $\gamma_0 = \gamma_n = 0$, which will be of use later [e.g. in Eq. (8.36)], do not occur in Eq. (8.23a).

The $2n$ values of the discrete function f_v are determined *exactly* in Eq. (8.21) by $n+1$ (generally nonzero) cosine amplitudes and by $n-1$ (generally nonzero) sine amplitudes. Looking ahead, we shall use Eqs. (8.21)-(8.23) to azimuthally decompose the quad-averaged radiances $L(\zeta;u,v)$ into spectral amplitudes, which we shall then find by invariant imbedding methods. The last step of our solution will be to use Eq. (8.21) to determine the quad-averaged radiances from the solution spectral amplitudes. Since this equation is exact, its use causes no loss of directional accuracy in the solution radiances. *The azimuthal resolution of the continuous radiance distribution $L(\zeta;\mu,\phi)$ is determined solely by the fineness of the directional resolution $\Delta\phi$ in the quad-averaging process.* The smallest scale of azimuthal variability resolved by quad averaging is given by the "two-point oscillation" corresponding to the $\cos(n\phi_v)$ term in Eq. (8.21); the "wavelength" of this two-point oscillation is $2\Delta\phi = 2\pi/n$.

Note that *each and every term in Eq. (8.21) must be included; there can be no truncation of this series.* This is in contrast to the Fourier analysis of continuous functions (which we shall discuss in Section 9.1).   In the continuous case, $L(\zeta;\mu,\phi)$ is represented by an infinite series, which is then truncated at a finite value of l in order to generate a finite number of equations for solution.   That approach leads to an approximate solution for the continuous radiance; *our approach leads to an exact solution for the quad-averaged radiances.* We choose the quad-averaged path because the quad-averaged radiances have a clear physical interpretation, and because the equations for the discrete spectral amplitudes can be solved with great numerical efficiency.

A few additional formulas for discrete functions will be needed below. Let g_{sv} be a discrete function of $\cos(\phi_s - \phi_v)$. Then

$$g_{sv} \equiv g\,[\cos(\phi_s - \phi_v)] \;=\; \sum_{l=0}^{n} \hat{g}(l)\cos[l(\phi_s - \phi_v)]\,, \qquad (8.24)$$

where

$$\hat{g}(l) \;=\; \frac{1}{\epsilon_l \cos(l\phi_s)} \sum_{v=1}^{2n} g_{sv}\cos(l\phi_v)\,. \qquad (8.25)$$

Since g_{sv} depends only on the difference $\phi_s - \phi_v$, we can set $s = 1$ without loss of generality; this merely anchors $\phi_s - \phi_v$ to $\phi_1 = 0$. This choice is motivated by the symmetry of the phase function, as expressed in Eqs. (5.7). Equations (8.24) and (8.25) will be applied to $\tilde{\beta}(\zeta; r, 1 \rightarrow u, v)$ as a function of ϕ_v.

Finally, we consider an arbitrary discrete function of two azimuthal angles ϕ_s and ϕ_v. Let $h_{sv} \equiv h(\phi_s, \phi_v)$, for $s, v = 1, 2, ..., 2n$. Then h_{sv} can be represented as

$$
\begin{aligned}
h_{sv} \;=\; & \sum_{k=0}^{n} \sum_{l=0}^{n} \hat{h}_{11}(k,l)\cos(k\phi_s)\cos(l\phi_v) \\
& + \sum_{k=0}^{n} \sum_{l=0}^{n} \hat{h}_{12}(k,l)\cos(k\phi_s)\sin(l\phi_v) \\
& + \sum_{k=0}^{n} \sum_{l=0}^{n} \hat{h}_{21}(k,l)\sin(k\phi_s)\cos(l\phi_v) \\
& + \sum_{k=0}^{n} \sum_{l=0}^{n} \hat{h}_{22}(k,l)\sin(k\phi_s)\sin(l\phi_v)\,.
\end{aligned}
\qquad (8.26)
$$

To find $\hat{h}_{11}(k,l)$, multiply Eq. (8.26) by $\cos(k'\phi_s)\cos(l'\phi_v)$, sum over s and v, and use the orthogonality relations (8.17)-(8.19). The other three amplitudes are found in an analogous manner. The results are

$$
\begin{aligned}
\hat{h}_{11}(k,l) \;&=\; \frac{1}{\epsilon_k\,\epsilon_l} \sum_{s=1}^{2n} \sum_{v=1}^{2n} h_{sv}\cos(k\phi_s)\cos(l\phi_v)\,, \\[4pt]
\hat{h}_{12}(k,l) \;&=\; \frac{1}{\epsilon_k\,\gamma_l} \sum_{s=1}^{2n} \sum_{v=1}^{2n} h_{sv}\cos(k\phi_s)\sin(l\phi_v)\,, \\[4pt]
\hat{h}_{21}(k,l) \;&=\; \frac{1}{\gamma_k\,\epsilon_l} \sum_{s=1}^{2n} \sum_{v=1}^{2n} h_{sv}\sin(k\phi_s)\cos(l\phi_v)\,, \\[4pt]
\hat{h}_{22}(k,l) \;&=\; \frac{1}{\gamma_k\,\gamma_l} \sum_{s=1}^{2n} \sum_{v=1}^{2n} h_{sv}\sin(k\phi_s)\sin(l\phi_v)\,.
\end{aligned}
\qquad (8.27)
$$

The arbitrary zero sine amplitudes $\hat{f}_2(0)$ and $\hat{f}_2(n)$ have their counterparts in the $\hat{h}$'s. In particular, we have

$$\hat{h}_{12}(k,0) = \hat{h}_{12}(k,n) = 0 \text{ for } k = 0, ..., n,$$

$$\hat{h}_{21}(0,l) = \hat{h}_{21}(n,l) = 0 \text{ for } l = 0, ..., n,$$

$$\hat{h}_{22}(0,0) = \hat{h}_{22}(n,n) = 0,$$

$$\hat{h}_{22}(n,0) = \hat{h}_{22}(0,n) = 0.$$

(8.28)

The special cases shown in Eq. (8.28) allow us to exclude any k or l values in Eq. (8.27) that would lead to a division by zero resulting from the γ_k or γ_l factors.

Equations (8.26)-(8.28) will be applied in Section 8.5 to the air-water surface transfer functions. We shall find that considerable simplification of these formulas can be obtained for air-water surfaces that have the symmetry expressed in Eqs. (4.42). For example, all $\hat{h}_{12}(k,l)$ and $\hat{h}_{21}(k,l)$ will turn out to be zero.

We now have at our disposal all of the tools necessary for converting the discrete physical Eqs. (8.8)-(8.11) into discrete spectral equations.

8.4 Discrete Spectral Form of the RTE ▐▌

It will be notationally convenient to write the quad-averaged RTE (8.10) as separate equations for *upward radiances*, $L^-(\zeta;u,v)$ where Q_{uv} is in Ξ_u, and for *downward radiances*, $L^+(\zeta;u,v)$ where Q_{uv} is in Ξ_d. The "+" and "−" superscripts are added to the radiances to denote which hemisphere, $\Xi_+ = \Xi_d$ or $\Xi_- = \Xi_u$, contains quad Q_{uv}.

In a similar fashion, a general function of (r,s) and (u,v) requires two superscripts. Thus, for the phase function $\tilde{\beta}(r,s{\rightarrow}u,v)$, we would write

$$\tilde{\beta}^{++}(r,s{\rightarrow}u,v) \text{ if } Q_{rs} \text{ is in } \Xi_+ \text{ and } Q_{uv} \text{ is in } \Xi_+,$$

$$\tilde{\beta}^{+-}(r,s{\rightarrow}u,v) \text{ if } Q_{rs} \text{ is in } \Xi_+ \text{ and } Q_{uv} \text{ is in } \Xi_-,$$

$$\tilde{\beta}^{-+}(r,s{\rightarrow}u,v) \text{ if } Q_{rs} \text{ is in } \Xi_- \text{ and } Q_{uv} \text{ is in } \Xi_+,$$

$$\tilde{\beta}^{--}(r,s{\rightarrow}u,v) \text{ if } Q_{rs} \text{ is in } \Xi_- \text{ and } Q_{uv} \text{ is in } \Xi_-.$$

However, the symmetries of the phase function expressed in Eqs. (5.7) imply that

$$\tilde{\beta}^{++}(r,s{\rightarrow}u,v) = \tilde{\beta}^{--}(r,s{\rightarrow}u,v) \equiv \tilde{\beta}^{+}(r,s{\rightarrow}u,v) \,,$$

$$\tilde{\beta}^{+-}(r,s{\rightarrow}u,v) = \tilde{\beta}^{-+}(r,s{\rightarrow}u,v) \equiv \tilde{\beta}^{-}(r,s{\rightarrow}u,v) \,. \tag{8.29}$$

The single superscripts on $\tilde{\beta}^{\pm}$ now denote scattering between quads within the same hemisphere, $\tilde{\beta}^{+}$, or scattering between quads in different hemispheres, $\tilde{\beta}^{-}$.

Using the superscript notation, the quad-averaged RTE (8.10) can be rewritten as a coupled pair of "upward" and "downward" differential equation systems:

$$\mp\mu_u \frac{dL^{\mp}(\zeta;u,v)}{d\zeta} = -L^{\mp}(\zeta;u,v)$$

$$+ \,\omega_o(\zeta) \sum_r \sum_s L^-(\zeta;r,s)\,\tilde{\beta}^{\pm}(\zeta;r,s{\rightarrow}u,v) \tag{8.30}$$

$$+ \,\omega_o(\zeta) \sum_r \sum_s L^+(\zeta;r,s)\,\tilde{\beta}^{\mp}(\zeta;r,s{\rightarrow}u,v) \,+\, \tilde{S}^{\mp}(\zeta;u,v) \,,$$

where now

$$\mu_u > 0\,, \qquad\qquad u,\, r \,=\, 1, 2, ..., m\,,$$

$$w \leq \zeta \leq m\,, \qquad\qquad v,\, s \,=\, 1, 2, ..., 2n\,.$$

and "$\sum_r\sum_s$" now *represents sums over the hemispheres indicated by the superscript on L.* (We presume that the reader will not confuse depth *m* with quad index *m*.) The *upper signs* are read together to generate equations governing the *upward radiances*, and the *lower signs correspond to the downward radiances.* Note that since we now take $\mu_u > 0$ always, the negative values of μ_u that occur in Eq. (8.10) when $Q_{uv} \in \Xi_- = \Xi_u$ are now accounted for by the minus sign in the $\mp\mu_u$ fact*or. This rewriting of the RTE into downward and upward parts will lead to equations that are similar in form to the two-flow equations for the downward and upward irradiances.*

Spectral decomposition of the RTE ▌▌

We can now proceed with the spectral decomposition of the RTE (8.30). We begin by writing

$$L^{\pm}(\zeta;u,v) \,=\, \sum_{l=0}^{n} \Big[\, \hat{L}_1^{\pm}(\zeta;u;l)\,\cos(l\phi_v) \,+\, \hat{L}_2^{\pm}(\zeta;u;l)\,\sin(l\phi_v)\,\Big]\,, \tag{8.31}$$

which holds for any depth and for all u and v values. This equation has the form of Eq. (8.21). We have added depth ζ and polar angle u arguments to the *cosine amplitudes for radiance*, $\hat{L}_1^{\pm}(\zeta;u;l)$, and to the *sine amplitudes for radiance*, $L_2^{\pm}(\zeta;u;l)$, in order to show their full functional form. These amplitudes, for fixed ζ and $u = 1, ..., m-1$, are determined by Eqs. (8.22) and (8.23), respectively, given the v-dependence of $L^{\pm}(\zeta;u,v)$.

The special case of the polar cap radiances $L^{\pm}(\zeta;m,\cdot)$ requires comment. Because the polar caps radiances have no ϕ dependence [recall the discussion leading to Eq. (4.62)], Eqs. (8.22) and (8.23) reduce to just

$$\hat{L}_1^{\pm}(\zeta;m;0) = L^{\pm}(\zeta;m,\cdot)$$

$$\hat{L}_1^{\pm}(\zeta;m;l) = 0 \quad \text{for } l = 1, ..., n \quad\quad\quad (8.32)$$

$$\hat{L}_2^{\pm}(\zeta;m;l) = 0 \quad \text{for } l = 0, ..., n .$$

Only the $l = 0$ cosine amplitude is non-zero. Thus we can regard Eq. (8.31) as holding for all quads and polar caps, if we remember that all amplitudes for polar caps are zero, except for the $l = 0$ cosine amplitude, which is equal to the radiance itself. Equations of the same form as (8.31) and (8.32) hold for the internal source terms $\tilde{S}$ and $\hat{S}$. For notational convenience, we omit the tilde on the spectral amplitude of $\tilde{\beta}$; i.e., $\hat{S} \equiv \hat{\tilde{S}}$. Likewise $\hat{\beta} \equiv \hat{\tilde{\beta}}$.

We next note that the quad-averaged phase function can be represented by

$$\tilde{\beta}^{\pm}(\zeta;r,1\rightarrow u,v) = \sum_{l=0}^{n} \hat{\beta}^{\pm}(\zeta;r,u;l) \cos(l\phi_v) , \quad\quad\quad (8.33)$$

where

$$\hat{\beta}^{\pm}(\zeta;r,u;l) = \frac{1}{\epsilon_l} \sum_{v=1}^{2n} \tilde{\beta}^{\pm}(\zeta;r,1\rightarrow u,v) \cos(l\phi_v) . \qu\quad\quad (8.34)$$

Formulas (8.33) and (8.34) correspond to Eqs. (8.24) and (8.25) tailored to the choice of $\phi_s = \phi_1 = 0$, as previously discussed.

Note that when $\tilde{\beta}^{\pm}$ is modeled as in Eq. (8.12), the depth dependence of the spectral amplitude $\hat{\beta}$ $\hat{\beta}^{\pm}$ resides in the scattering coefficient, just as does the depth dependence of the total $\tilde{\beta}$ in Eq. (8.12). Thus in practice we need evaluate Eq. (8.34) only once for a given scattering constituent. We retain the depth argument ζ in the total $\hat{\beta}$ $\hat{\beta}^{\pm}$ to remind ourselves that the spectral phase function amplitudes in general vary with depth.

There are actually four separate cases to be considered in the use of Eq. (8.34). These are as follows:

(i) Quad-to-quad scattering: $u, r = 1, 2, ..., m-1$. Eq. (8.34) holds as written.

(ii) Polar cap-to-quad scattering: $r = m$; $u = 1, 2, ..., m-1$. Eq. (8.34) reduces to

$$\hat{\beta}^{\pm}(\zeta;m,u;0) = \tilde{\beta}^{\pm}(\zeta;m,\cdot \to u,1)$$

$$\hat{\beta}^{\pm}(\zeta;m,u;l) = 0 \quad \text{if } l = 1, ..., n.$$

(iii) Quad-to-polar cap scattering: $r = 1, 2, ..., m-1$; $u = m$. Eq. (8.34) reduces to

$$\hat{\beta}^{\pm}(\zeta;r,m;0) = \tilde{\beta}^{\pm}(\zeta,r,1 \to m,\cdot)$$

$$\hat{\beta}^{\pm}(\zeta;r,m;l) = 0 \quad \text{if } l = 1, ..., n.$$

(iv) Polar cap-to-polar cap scattering: $r = m$; $u = m$. Eq. (8.34) reduces to

$$\hat{\beta}^{\pm}(\zeta;m,m;0) = \tilde{\beta}^{\pm}(\zeta;m,\cdot \to m,\cdot)$$

$$\hat{\beta}^{\pm}(\zeta;m,m;l) = 0 \quad \text{if } l = 1, ..., n.$$

We now substitute representation (8.31) for the quad-averaged radiances and effective source, and Eq. (8.33) for the phase function, into the RTE (8.30). For brevity, let us explicitly consider only the case of a non-polar-cap output quad Q_{uv}; i.e., $u = 1, ..., m-1$. Then Eq. (8.30) becomes

$$\mp \mu_u \frac{d}{d\zeta} \left\{ \sum_{l=0}^{n} \left[\hat{L}_1^{\mp}(\zeta;u;l) \cos(l\phi_v) + \hat{L}_2^{\mp}(\zeta;u;l) \sin(l\phi_v) \right] \right\}$$

$$= - \sum_{l=0}^{n} \left[\hat{L}_1^{\mp}(\zeta;u;l) \cos(l\phi_v) + \hat{L}_2^{\mp}(\zeta;u;l) \sin(l\phi_v) \right]$$

$$+ \omega_o(\zeta) \sum_{r=1}^{m-1} \sum_{s=1}^{2n} \sum_{l=0}^{n} \left[\hat{L}_1^{-}(\zeta;r;l) \cos(l\phi_s) + \hat{L}_2^{-}(\zeta;r;l) \sin(l\phi_s) \right] \times$$

$$\left[\sum_{k=0}^{n} \hat{\beta}^{\pm}(\zeta;r,u;k) \cos k(\phi_s - \phi_v) \right]$$

$$+ \omega_o(\zeta) \hat{L}_1^{-}(\zeta;m;0) \hat{\beta}^{\pm}(\zeta;m,u;0) \tag{8.35}$$

$$+ \omega_o(\zeta) \sum_{r=1}^{m-1} \sum_{s=1}^{2n} \sum_{l=0}^{n} \left[\hat{L}_1^+(\zeta;r;l) \cos(l\phi_s) + \hat{L}_2^+(\zeta;r;l) \sin(l\phi_s) \right] \times$$

$$\left[\sum_{k=0}^{n} \hat{\beta}^{\mp}(\zeta;r,u;k) \cos k(\phi_s - \phi_v) \right]$$

$$+ \omega_o(\zeta) \hat{L}_1^+(\zeta;m,0) \hat{\beta}^{\mp}(\zeta;m,u;0)$$

$$+ \sum_{l=0}^{n} \left[\hat{S}_1^{\mp}(\zeta;u;l) \cos(l\phi_v) + \hat{S}_2^{\mp}(\zeta;u;l) \sin(l\phi_v) \right].$$

In going from Eq. (8.30) to (8.35), the summations over all *r, s* have been written as in Eq. (4.62) to explicitly show the polar cap terms.

The second and fourth terms on the right-hand side of Eq. (8.35) each have the form

$$\omega_o(\zeta) \sum_{r=1}^{m-1} \sum_{l=0}^{n} \sum_{k=0}^{n} \hat{L}_1(\zeta;r;l) \hat{\beta}(\zeta;r,u;k) \left[\sum_{s=1}^{2n} \cos(l\phi_s) \cos k(\phi_s - \phi_v) \right]$$

$$+ \omega_o(\zeta) \sum_{r=1}^{m-1} \sum_{l=0}^{n} \sum_{k=0}^{n} \hat{L}_2(\zeta;r;l) \hat{\beta}(\zeta;r,u;k) \left[\sum_{s=1}^{2n} \sin(l\phi_s) \cos k(\phi_s - \phi_v) \right].$$

Application of Eqs. (8.20) to the sums over *s*, and use of Eqs. (8.22b) and (8.23b), reduces these terms to a simpler form. Moreover, the polar cap terms can be viewed as coefficients of $\cos(l\phi_v)$ for $l = 0$, and as such they can be incorporated into the other summations. Equation (8.35) thus reduces to

$$\mp \mu_u \sum_{l=0}^{n} \left[\frac{d\hat{L}_1^{\mp}(\zeta;u;l)}{d\zeta} \cos(l\phi_v) + \frac{d\hat{L}_2^{\mp}(\zeta;u;l)}{d\zeta} \sin(l\phi_v) \right]$$

$$= - \sum_{l=0}^{n} \left[\hat{L}_1^{\mp}(\zeta;u;l) \cos(l\phi_v) + \hat{L}_2^{\mp}(\zeta;u;l) \sin(l\phi_v) \right]$$

$$+ \omega_o(\zeta) \sum_{l=0}^{n} \left[\sum_{r=1}^{m-1} \hat{L}_1^-(\zeta;r;l) \hat{\beta}^{\pm}(\zeta;r,u;l) \epsilon_l + \hat{L}_1^-(\zeta;m;l) \hat{\beta}^{\pm}(\zeta;m,u;l) \delta_l \right] \cos(l\phi_v)$$

$$+ \omega_o(\zeta) \sum_{l=0}^{n} \left[\sum_{r=1}^{m-1} \hat{L}_2^-(\zeta;r;l) \hat{\beta}^{\pm}(\zeta;r,u;l) \gamma_l \right] \sin(l\phi_v)$$

$$(8.36)$$

$$+ \omega_o(\zeta) \sum_{l=0}^{n} \left[\sum_{r=1}^{m-1} \hat{L}_1^+(\zeta;r;l)\, \hat{\beta}^\mp(\zeta;r,u;l)\, \epsilon_l \; + \; \hat{L}_1^+(\zeta;m;l)\, \hat{\beta}^\mp(\zeta;m,u;l)\, \delta_l \right] \cos(l\phi_v)$$

$$+ \omega_o(\zeta) \sum_{l=0}^{n} \left[\sum_{r=1}^{m-1} \hat{L}_2^+(\zeta;r;l)\, \hat{\beta}^\mp(\zeta;r,u;l)\, \gamma_l \right] \sin(l\phi_v)$$

$$+ \sum_{l=0}^{n} \left[\hat{S}_1^\mp(\zeta;u;l) \cos(l\phi_v) \; + \; \hat{S}_2^\mp(\zeta;u;l) \sin(l\phi_v) \right].$$

We now take advantage of the linear independence of $\cos(l\phi_v)$ and $\sin(l\phi_v)$ for different l values to observe that *this last equation must hold true for each value l = 0, ..., n for the $\hat{L}_1$ and for l = 1, ...,n−1 for the $\hat{L}_2$ amplitudes separately.* Accordingly, collecting together and equating the coefficients of $\cos(l\phi_v)$ in Eq. (8.36) gives

$$\mp \mu_u \frac{d}{d\zeta} \hat{L}_1^\mp(\zeta;u;l) \; = \; - \hat{L}_1^\mp(\zeta;u;l)$$

$$+ \omega_o(\zeta)\, \epsilon_l \sum_{r=1}^{m-1} \hat{L}_1^-(\zeta;r;l)\, \hat{\beta}^\pm(\zeta;r,u;l) \; + \; \omega_o(\zeta)\, \delta_l\, \hat{L}_1^-(\zeta;m;l)\, \hat{\beta}^\pm(\zeta;m,u;l)$$

$$+ \omega_o(\zeta)\, \epsilon_l \sum_{r=1}^{m-1} \hat{L}_1^+(\zeta;r;l)\, \hat{\beta}^\mp(\zeta;r,u;l) \; + \; \omega_o(\zeta)\, \delta_l\, \hat{L}_1^+(\zeta;m;l)\, \hat{\beta}^\mp(\zeta;m,u;l)$$

$$+ \hat{S}_1^\mp(\zeta;u;l).$$

(8.37)

Equation (8.37) holds for all $w \le \zeta \le m$; $u = 1, ..., m−1$; $l = 0, ..., n$; and $\mu_u > 0$.

Collecting together and equating the coefficients of $\sin(l\phi_v)$ on each side of Eq. (8.36) for $l = 1, ..., n−1$ gives a similar equation for the sine amplitudes:

$$\mp \mu_u \frac{d}{d\zeta} \hat{L}_2^\mp(\zeta;u;l) \; = \; - \hat{L}_2^\mp(\zeta;u;l)$$

$$+ \omega_o(\zeta)\, \gamma_l \sum_{r=1}^{m-1} \hat{L}_2^-(\zeta;r;l)\, \hat{\beta}^\pm(\zeta;r,u;l)$$

$$+ \omega_o(\zeta)\, \gamma_l \sum_{r=1}^{m-1} \hat{L}_2^+(\zeta;r;l)\, \hat{\beta}^\mp(\zeta;r,u;l)$$

$$+ \hat{S}_2^\mp(\zeta;u;l),$$

(8.38)

which holds for $w \le \zeta \le m$; $u = 1, ..., m−1$; $l = 1, ..., n−1$; and $\mu_u > 0$.

Since $\hat{L}_2^{\pm}(\zeta;u;l) \equiv 0$ when $l = 0$ or $l = n$, and with the same statement for $\hat{S}_2^{\pm}(\zeta;u;l)$, we can regard Eq. (8.38) as formally holding for the full range of values, $l = 0, 1, ..., n$.

We now must return to Eq. (8.30) and repeat the above reduction for the case of a polar-cap output quad, i.e. $(u,v) = (m,\cdot)$. We shall leave this exercise to the reader. The polar-cap equation corresponding to Eq. (8.37) is

$$\mp\mu_m \frac{d}{d\zeta} \hat{L}_1^{\mp}(\zeta;m;0) = -\hat{L}_1^{\mp}(\zeta;m;0)$$

$$+ \omega_o(\zeta) \, \epsilon_0 \sum_{r=1}^{m-1} \hat{L}_1^-(\zeta;r;0) \, \hat{\beta}^{\pm}(\zeta;r,m;0) + \omega_o(\zeta) \, \hat{L}_1^-(\zeta;m;0) \, \hat{\beta}^{\pm}(\zeta;m,m;0)$$

$$\tag{8.39}$$

$$+ \omega_o(\zeta) \, \epsilon_0 \sum_{r=1}^{m-1} \hat{L}_1^+(\zeta;r;0) \, \hat{\beta}^{\mp}(\zeta;r,m;0) + \omega_o(\zeta) \, \hat{L}_1^+(\zeta;m;0) \, \hat{\beta}^{\mp}(\zeta;m,m;0)$$

$$+ \hat{S}_1^{\mp}(\zeta;m;0) \, .$$

There is no polar-cap equation corresponding to Eq. (8.38), because the sine amplitudes are all zero for polar caps.

Equations (8.37)-(8.39) constitute the spectral form of the RTE (8.30). We can rewrite these equations in a more convenient matrix form as follows. We shall explicitly consider only Eq. (8.37). Writing Eq. (8.37) as separate equations for the downward (+) and upward(−) cases, dividing by μ_u, and rearranging terms, gives

$$\frac{d}{d\zeta} \hat{L}_1^+(\zeta;u;l) = \sum_{r=1}^{m-1} \hat{L}_1^-(\zeta;r;l) \left[\frac{\omega_o(\zeta) \, \epsilon_l \, \hat{\beta}^-(\zeta;r,u;l)}{\mu_u} \right]$$

$$+ \hat{L}_1^-(\zeta;m;l) \left[\frac{\omega_o(\zeta) \, \delta_l \, \hat{\beta}^-(\zeta;m,u;l)}{\mu_u} \right]$$

$$\tag{8.40}$$

$$+ \sum_{r=1}^{m-1} \hat{L}_1^+(\zeta;r;l) \left[\frac{\omega_o(\zeta) \, \epsilon_l \, \hat{\beta}^+(\zeta;r,u;l)}{\mu_u} - \frac{\delta_{r-u}}{\mu_u} \right]$$

$$+ \hat{L}_1^+(\zeta;m;l) \left[\frac{\omega_o(\zeta) \, \delta_l \, \hat{\beta}^+(\zeta;m,u;l)}{\mu_u} \right] + \frac{\hat{S}_1^+(\zeta;u;l)}{\mu_u}$$

for the downward case, where $u = 1, ..., m-1$ and $l = 0, ..., n$. For the upward case we get

$$-\frac{d}{d\zeta}\hat{L}_1^-(\zeta;u;l) = \sum_{r=1}^{m-1}\hat{L}_1^-(\zeta;r;l)\left[\frac{\omega_o(\zeta)\,\epsilon_l\,\hat{\beta}^+(\zeta;r,u;l)}{\mu_u} - \frac{\delta_{r-u}}{\mu_u}\right]$$

$$+ \hat{L}_1^-(\zeta;m;l)\left[\frac{\omega_o(\zeta)\,\delta_l\,\hat{\beta}^+(\zeta;m,u;l)}{\mu_u}\right]$$

$$+ \sum_{r=1}^{m-1}\hat{L}_1^+(\zeta;r;l)\left[\frac{\omega_o(\zeta)\,\epsilon_l\,\hat{\beta}^-(\zeta;r,u;l)}{\mu_u}\right] \qquad (8.41)$$

$$+ \hat{L}_1^+(\zeta;m;l)\left[\frac{\omega_o(\zeta)\,\delta_l\,\hat{\beta}^-(\zeta;m,u;l)}{\mu_u}\right] + \frac{\hat{S}_1^-(\zeta;u;l)}{\mu_u}.$$

where $u = 1, ..., m-1$ and $l = 0, ..., n$. Similar equations can be obtained from Eqs. (8.38) and (8.39).

The quantities in square brackets in Eqs. (8.40) and (8.41) are the *spectral local reflectance* and *spectral local transmittance functions for the radiance amplitudes* $\hat{L}_1^\pm(\zeta;u;l)$. *Note that these quantities depend only on the IOP's at depth ζ and on the choice of quad-partioning schemes.* Note also that the *same* bracketed quantities appear in both the downward and upward equations.

Our immediate goal is the construction of an *m×m spectral local reflectance matrix* $\hat{\rho}(\zeta;l)$ and an *m×m spectral local transmittance matrix* $\hat{t}(\zeta;l)$ for $l = 0, 1,..., n$ and for each depth ζ. Let the elements of the rth row and u^{th} column of these matrices be denoted by $[\hat{\rho}(\zeta;l)]_{ru}$ and $[\hat{t}(\zeta;l)]_{ru}$, respectively. Moreover, recall that $\epsilon_l = \gamma_l = n$ when l is the range $l = 1, ..., n-1$, and that $\gamma_l = 0$ for $l = 0$ and $l = n$. Then we define the matrix elements as follows:

(i) Quad-to-quad case ($r, u = 1, ..., m-1$):

$$[\hat{t}(\zeta;l)]_{ru} \equiv [\epsilon_l\,\omega_o(\zeta)\,\hat{\beta}^+(\zeta;r,u;l) - \delta_{r-u}]/\mu_u$$

$$[\hat{\rho}(\zeta;l)]_{ru} \equiv \epsilon_l\,\omega_o(\zeta)\,\hat{\beta}^-(\zeta;r,u;l)/\mu_u \qquad (8.42a)$$

$$\text{for } l = 0, ..., n.$$

(ii) Polar cap-to-quad case ($r = m; u = 1, ..., m-1$):

$$[\hat{t}(\zeta;l)]_{mu} \equiv \delta_l\,\omega_o(\zeta)\,\hat{\beta}^+(\zeta;m,u;l)/\mu_u$$

$$[\hat{\rho}(\zeta;l)]_{mu} \equiv \delta_l\,\omega_o(\zeta)\,\hat{\beta}^-(\zeta;m,u;l)/\mu_u \qquad (8.42b)$$

$$\text{for } l = 0, ..., n.$$

(iii) Quad-to-polar cap case ($r = 1, ..., m-1$; $u = m$):

$$[\hat{\underline{t}}(\zeta;0)]_{rm} \equiv \epsilon_0\, \omega_o(\zeta)\, \hat{\beta}^+(\zeta;r,m;0)/\mu_m$$

$$[\hat{\underline{t}}(\zeta;l)]_{rm} \equiv 0 \quad \text{for } l = 1, ..., n$$

$$[\hat{\underline{\rho}}(\zeta;0)]_{rm} \equiv \epsilon_0\, \omega_o(\zeta)\, \hat{\beta}^-(\zeta;r,m;0)/\mu_m$$

$$[\hat{\underline{\rho}}(\zeta;l)]_{rm} \equiv 0 \quad \text{for } l = 1, ..., n\,.$$

(8.42c)

(iv) Polar cap-to-polar cap case ($r = m$; $u = m$):

$$[\hat{\underline{t}}(\zeta;0)]_{mm} \equiv [\omega_o(\zeta)\, \hat{\beta}^+(\zeta;m,m;0) - 1]/\mu_m$$

$$[\hat{\underline{t}}(\zeta;l)]_{mm} \equiv 0 \quad \text{for } l = 1, ..., n$$

$$[\hat{\underline{\rho}}(\zeta;0)]_{mm} \equiv \omega_o(\zeta)\, \hat{\beta}^-(\zeta;m,m;0)/\mu_m$$

$$[\hat{\underline{\rho}}(\zeta;l)]_{mm} \equiv 0 \quad \text{for } l = 1, ..., n\,.$$

(8.42d)

Note that the mth row and m^{th} column of $\hat{\underline{t}}$ and $\hat{\underline{\rho}}$ are zero, except when $l = 0$. This corresponds to the fact that only the $l = 0$ cosine amplitude is nonzero for polar caps, $r = m$ or $u = m$.

With definitions (8.42), Eqs. (8.40) and (8.41) become

$$\frac{d}{d\zeta}\, \hat{L}_1^+(\zeta;u;l) = \sum_{r=1}^{m} \hat{L}_1^-(\zeta;r;l)\, [\hat{\underline{\rho}}(\zeta;l)]_{ru}$$

$$+ \sum_{r=1}^{m} \hat{L}_1^+(\zeta;r;l)\, [\hat{\underline{t}}(\zeta;l)]_{ru} + \hat{S}_1^+(\zeta;u,l)/\mu_u\,,$$

(8.43a)

and

$$-\frac{d}{d\zeta}\, \hat{L}_1^-(\zeta;u;l) = \sum_{r=1}^{m} \hat{L}_1^-(\zeta;r;l)\, [\hat{\underline{t}}(\zeta;l)]_{ru}$$

$$+ \sum_{r=1}^{m} \hat{L}_1^+(\zeta;r;l)\, [\hat{\underline{\rho}}(\zeta;l)]_{ru} + \hat{S}_1^-(\zeta;u;l)/\mu_u\,.$$

(8.43b)

These equations are valid for $l = 0, ..., n$ and for $u = 1, ..., m-1$. Note that the "attenuation" terms [the first terms on the right-hand sides of Eqs. (8.37) and (8.39)] have been incorporated into the local transmittance functions when $r = u$. The polar-cap Eq. (8.39) leads to a similar pair of equations involving $[\hat{\underline{t}}(\zeta;0)]_{rm}$ and $[\hat{\underline{\rho}}(\zeta;0)]_{rm}$.

These cosine amplitude equations can be combined by defining the $1 \times m$ matrices

$$\hat{\underline{L}}_1^{\pm}(\zeta;l) \equiv [\hat{L}_1^{\pm}(\zeta;1;l), ..., \hat{L}_1^{\pm}(\zeta;m-1;l), \hat{L}_1^{\pm}(\zeta;m;l)] \qquad (8.44a)$$

and

$$\hat{\underline{S}}_1^{\pm}(\zeta;l) \equiv [\hat{S}_1^{\pm}(\zeta;1;l)/\mu_1, ..., \hat{S}_1^{\pm}(\zeta;m-1;l)/\mu_{m-1}, \hat{S}_1^{\pm}(\zeta;m;l)/\mu_m] . \qquad (8.44b)$$

Note that by virtue of Eq. (8.32), the last elements of $\hat{\underline{L}}_1^{\pm}$ and $\hat{\underline{S}}_1^{\pm}$ are nonzero only when $l = 0$. The cosine amplitude equations now read

$$\mp \frac{d}{d\zeta} \hat{\underline{L}}_1^{\mp}(\zeta;l) = \hat{\underline{L}}_1^{\mp}(\zeta;l) \, \hat{\underline{t}}(\zeta;l) + \hat{\underline{L}}_1^{\pm}(\zeta;l) \, \hat{\underline{\rho}}(\zeta;l) + \hat{\underline{S}}_1^{\mp}(\zeta;l) . \qquad (8.45)$$

The sine amplitude equations can be placed in the same form as Eq. (8.45). Strictly speaking, the $\hat{\underline{t}}$ and $\hat{\underline{\rho}}$ matrices for the sine amplitude equations are $(m-1) \times (m-1)$, because the polar-cap sine amplitudes are always zero. Likewise, the vectors $\hat{\underline{L}}_2^{\pm}(\zeta;l)$ and $\hat{\underline{S}}_2^{\pm}(\zeta;l)$ corresponding to Eq. (8.44) are nonzero only for $l = 1, ..., n-1$. However, it is notationally convenient to fill out $\hat{\underline{t}}$ and $\hat{\underline{\rho}}$ with a bottom row and right column of zeros, and to set $\hat{\underline{L}}_2^{\pm}(\zeta;l) = \underline{0}_{1 \times m}$ and $\hat{\underline{S}}_2^{\pm}(\zeta;l) = \underline{0}_{1 \times m}$ for $l = 0$ and $l = n$. Then both the cosine and sine amplitudes can be combined into one set of equations:

$$\mp \frac{d}{d\zeta} \hat{\underline{L}}_p^{\mp}(\zeta;l) = \hat{\underline{L}}_p^{\mp}(\zeta;l) \, \hat{\underline{t}}(\zeta;l) + \hat{\underline{L}}_p^{\pm}(\zeta;l) \, \hat{\underline{\rho}}(\zeta;l) + \hat{\underline{S}}_p^{\mp}(\zeta;l) , \qquad (8.46)$$

where $p = 1$ or 2; $l = 0, 1, ..., n$; and $w \le \zeta \le m$. Here the $\hat{\underline{L}}_p^{\pm}$ and $\hat{\underline{S}}_p^{\pm}$ are all $1 \times m$ matrices defined by Eq. (8.44), and $\hat{\underline{t}}$ and $\hat{\underline{\rho}}$ are $m \times m$ matrices whose elements are given by Eqs. (8.42). The forms of these equations for the downward and upward radiance amplitudes should be compared with Eqs. (7.3) and (7.4) for the downward and upward irradiances.

Equations (8.46) are the *local interaction equations for the radiance amplitudes.* Several important features of these equations should be noted:

- *The sets of equations for different l-modes, l = 0, 1, ..., n, are independent.* This permits a considerable savings in computer requirements, since we can solve a sequence of $n+1$ "small" problems, rather than one "large" problem. Indeed, *this decoupling of the azimuthal modes is the primary reason for decomposing the radiance equations into spectral form.*

- *The "information content" of the amplitude equations is the same as for the radiance equations.* The number of nonzero amplitudes for either upward or downward radiances is

m	for $p = 1$ and $l = 0$,
$(m-1)n$	for $p = 1$ and $l = 1, ..., n$,
$(m-1)(n-1)$	for $p = 2$ and $l = 1, ..., n-1$.

  But $m + (m-1)n + (m-1)(n-1) = (m-1)2n + 1$, which is exactly the number of quads for which $L^{\pm}(\zeta;u,v)$ must be determined in either the upward or the downward hemispheres [namely, $(m-1)$ bands of $2n$ ϕ-quads, plus a polar cap]. However, the radiance Eqs. (8.30) must be solved simultaneously as one "large" problem.

- *The radiance-amplitude matrix equations have almost exactly the same mathematical form as the two-flow equations.* Therefore, *the invariant imbedding methods developed in Chapter 7 are easily adapted to the solution of Eqs. (8.46).*

- The *local transmittance and reflectance matrices $\hat{\underline{t}}$ and $\hat{\underline{\rho}}$ are inherent optical properties.* Note in particular that the same $\hat{\underline{t}}$ and $\hat{\underline{\rho}}$ are used in both the upward and downward amplitude equations. This stands in contrast to the two-flow equations, which had different τ's and ρ's for the upward and downward equations, because the irradiance τ's and ρ's are apparent optical properties. *In this very important sense, then, the radiance-amplitude equations are even simpler than the two-flow equations.*

8.5   Discrete Spectral Forms of the Boundary Conditions ▐▌

Before proceeding with the solution of the radiance amplitude Eqs. (8.46), we must place the quad-averaged boundary conditions on an equal footing. We shall note only the highlights of this process, since it parallels the spectral decomposition of the RTE itself.

Implications of surface-wave symmetries ▌▌

    The four quad-averaged, air-water surface transfer functions $t(a,x;r,s \rightarrow u,v)$, etc., are in general each represented by equations of the form (8.26). Such a representation can describe any air-water surface. However, if the surface wave spectrum exhibits symmetry about the wind direction, important simplifications can be achieved. We shall illustrate the simplification process for the case of capillary waves, which have the elliptical symmetry expressed by Eqs. (4.42).

    Consider, for example, the $\hat{t}_{12}$ term, which is patterned after the $\hat{h}_{12}$ term of Eq. (8.27):

$$\hat{t}_{12}(a,w;r,k|u,l) \equiv \frac{1}{\epsilon_k \gamma_l} \sum_{s=1}^{2n} \sum_{v=1}^{2n} t(a,w;r,s \rightarrow u,v) \cos(k\varphi_s) \sin(l\varphi_v) \,.$$

In our quad indexing scheme, $\varphi_{2n+2-w} = 2\pi - \varphi_w$. Therefore Eq. (4.42a) implies that

$$\hat{t}_{12}(a,w;r,k|u,l) =$$
$$\frac{1}{\epsilon_k \gamma_l} \sum_{s=1}^{2n} \sum_{v=1}^{2n} t(a,w;r,2n+2-s \rightarrow u,2n+2-v) \cos(l\varphi_s) \sin(l\varphi_v) \,.$$

Changing summation indices to $s' \equiv 2n+2-s$ and $v' \equiv 2n+2-v$ gives

$$\hat{t}_{12}(a,w;r,k|u,l) =$$
$$\frac{1}{\epsilon_k \gamma_l} \sum_{s'=2n+1}^{2} \sum_{v'=2n+1}^{2} t(a,w;r,s' \rightarrow u,v') \cos(k\varphi_{2n+2-s'}) \sin(l\varphi_{2n+2-v'}) \,.$$

Noting once again that $\varphi_{2n+2-w} = 2\pi - \varphi_w$ and using the evenness of the cosine and the oddness of the sine gives

$$\hat{t}_{12}(a,w;r,k|u,l) = \frac{1}{\epsilon_k \gamma_l} \sum_{s'=2n+1}^{2} \sum_{v'=2n+1}^{2} t(a,w;r,s' \rightarrow u,v') \cos(k\varphi_{s'}) [-\sin(l\varphi_{v'})] \,.$$

Remembering that quad $s = 2n+1$ is the same quad as $s = 1$, and reordering sums, gives

$$\hat{t}_{12}(a,w;r,k|u,l) = -\frac{1}{\epsilon_k \gamma_l} \sum_{s'=1}^{2n} \sum_{v'=1}^{2n} t(a,w;r,s' \rightarrow u,v') \cos(k\varphi_{s'}) \sin(l\varphi_{s'})$$
$$= -\hat{t}_{12}(a,w;r,k|u,l) \,.$$

Therefore it follows that

$$\hat{t}_{12}(a,w;r,k|u,l) \; = \; 0 \, ,$$

for r, $u = 1, ..., m$ and k, $l = 0, ..., n$.

An identical analysis shows that $\hat{t}_{21}(a,w;r,k|u,l) \; = \; 0$ over the full r, k, u, l ranges, and the same results are found for the other three reflectance and transmittance functions. Thus *the elliptical symmetry of the surface about the wind direction eliminates two of the four terms in Eq.* (8.27).

A similar sort of analysis [using Eq. (4.42b)] leads to the result

$$\hat{t}_{11}(a,w;r,k|u,l) \; = \; (-1)^{k+l} \frac{1}{\epsilon_k \epsilon_l} \sum_{s'=1}^{2n} \sum_{v'=1}^{2n} t(a,w;r,s'{\rightarrow}u,v') \cos(k\phi_{s'}) \cos(l\phi_{v'})$$

$$= \; (-1)^{k+l} \hat{t}_{11}(a,w;r,k|u,l) \, .$$

Therefore it follow that

$$\hat{t}_{11}(a,w;r,k|u,l) \; = \; 0 \quad \text{if } k+l \text{ is odd}, \tag{8.47}$$

for r, $u = 1, 2, ..., m$ and k, $l = 0, ..., n$. Corresponding results are obtained for $\hat{t}_{22}$ and for the other three surface transfer functions.

We can therefore simplify the notation to one subscript for the $\hat{t}$ and $\hat{r}$ functions, e.g.

$$\hat{t}_1(a,w;r,k|u,l) \; \equiv \; \hat{t}_{11}(a,w;r,k|u,l)$$

$$\hat{t}_2(a,w;r,k|u,l) \; \equiv \; \hat{t}_{22}(a,w;r,k|u,l) \, ,$$

since the terms with subscripts 12 and 21 are always zero. We can now represent the surface transfer functions by spectral equations of the form

$$t(a,w;r,s{\rightarrow}u,v) \; = \; \sum_{k=0}^{n} \sum_{l=0}^{n} \hat{t}_1(a,w;r,k|u,l) \cos(k\phi_s)\cos(l\phi_v)$$

$$\tag{8.48}$$

where
$$+ \; \sum_{k=0}^{n} \sum_{l=0}^{n} \hat{t}_2(a,w;r,k|u,l) \sin(k\phi_s) \sin(l\phi_v) \, ,$$

$$\hat{t}_1(a,w;r,k|u,l) \; = \; \frac{1}{\epsilon_k \epsilon_l} \sum_{s=1}^{2n} \sum_{v=1}^{2n} t(a,w;r,s{\rightarrow}u,v) \cos(k\phi_s) \cos(l\phi_v) \, ,$$

$$\tag{8.49a}$$

$$\text{for } k, \; l \; = \; 0, ..., n \, ,$$

and where

$$
\hat{t}_2(a,w;r,k|u,l) = \begin{cases} \dfrac{1}{\gamma_k \gamma_l} \displaystyle\sum_{s=1}^{2n} \sum_{v=1}^{2n} t(a,w;r,s\rightarrow u,v) \sin(k\phi_s) \sin(l\phi_v), \\[4pt] \qquad \text{if } k, l = 1, ..., n-1 \\[6pt] 0, \quad \text{if } k = 0 \quad \text{and} \quad l = 0, ..., n \\[6pt] 0, \quad \text{if } l = 0 \quad \text{and} \quad k = 0, ..., n. \end{cases}
\tag{8.49b}
$$

As just noted, Eqs. (8.48) and (8.49) are nontrivial only when $k+l$ is even.

The simplifications that we have just obtained in the air-water surface transfer functions result in a major computational savings. The dual origins of the results should be noted. First, we assumed that the surface wave spectrum has an elliptical symmetry about the wind direction, and second, we chose a wind-oriented coordinate system. Had we not had the foresight to choose a wind-oriented coordinate system in Section 4.1, we could not have expressed the elliptical symmetry in a mathematically useful form.

The capillary and gravity wave spectra discussed in Chapter 4 possess the assumed symmetry. However, nature can without difficulty generate wave patterns that have no symmetry about the wind direction. Such a situation occurs, for example. if swell is running at an angle to the locally wind-generated seas. In such situations, all of the $\hat{t}_{12}(a,w;r,k|u,l)$, $\hat{t}_{21}(a,w;r,k|u,l)$, etc., are nonzero and must be retained in the calculations.

Spectral decomposition of the surface boundary conditions ▌▌

We now return to the quad-averaged surface boundary conditions (8.8) and (8.9). In these equations, we replace the quad-averaged radiances by spectral representations of the form of Eq. (8.31), and the r's and t's are represented as in Eq. (8.48). As always, the polar-cap quads require special treatment. The reduction of the equations makes use of the orthogonality relations and the linear independence of the cosines and sines. The reader may find it amusing to perform this derivation, following in parallel the steps seen in Section 8.4, but we would not. We therefore only state the results needed later.

It proves convenient to define the elements of an $m \times m$ matrix $\hat{\underline{t}}_1(a,w;k|l)$ by

$$
[\hat{\underline{t}}_1(a,w;k|l)]_{ru} \equiv \begin{cases} \epsilon_k \hat{t}_1(a,w;r,k|u,l) & \text{for } r = 1, ..., m-1 \\[6pt] \delta_k \hat{t}_1(a,w;r,k|u,l) & \text{for } r = m, \end{cases}
\tag{8.50}
$$

which holds for $u = 1, ..., m$ and $k, l = 0, ..., n$. The other three $\underline{\hat{r}}_1$ and $\underline{\hat{t}}_1$ matrices have corresponding definitions. Likewise, we define the elements of an $m \times m$ matrix $\underline{\hat{t}}_2(a,w;k|l)$ by

$$[\underline{\hat{t}}_2(a,w;k|l)]_{ru} \equiv \begin{cases} \gamma_k \, \hat{t}_2(a,w;r,k|u,l) & \text{for } r = 1, ..., m-1 \\ & \text{and } l = 1, ..., n-1 \\ 0 & \text{for } r = m \\ & \text{or } l = 0 \text{ or } l = n. \end{cases} \tag{8.51}$$

which holds for $u = 1, ..., m$ and $k = 0, ..., n$. The other $\underline{\hat{r}}_2$ and $\underline{\hat{t}}_2$ matrices have corresponding definitions.

Many of the elements of the various $\underline{\hat{t}}$ and $\underline{\hat{r}}$ matrices are zero by virtue of the polar-cap special cases, and because of results such as Eq. (8.47), which gives non-zero values only when $k+l$ is an even integer. An explicit presentation of all quantities is given in Mobley and Preisendorfer (1988).

With definitions (8.50) and (8.51), we can now write the spectral, matrix forms of the air-water surface boundary conditions. Equation (8.8) becomes

$$\underline{\hat{L}}_p^-(a;l) = \sum_{\substack{k=0 \\ (k+l \text{ even})}}^{n} \underline{\hat{L}}_p^-(w;k) \, \underline{\hat{t}}_p(w,a;k|l) + \sum_{\substack{k=0 \\ (k+l \text{ even})}}^{n} \underline{\hat{L}}_p^+(a;k) \, \underline{\hat{r}}_p(a,w;k|l), \tag{8.52}$$

where $p = 1$ or 2 and $l = 0, ..., $ n. Equation (8.9) becomes

$$\underline{\hat{L}}_p^+(w;l) = \sum_{\substack{k=0 \\ (k+l \text{ even})}}^{n} \underline{\hat{L}}_p^-(w;k) \, \underline{\hat{r}}_p(w,a;k|l) + \sum_{\substack{k=0 \\ (k+l \text{ even})}}^{n} \underline{\hat{L}}_p^+(a;k) \, \underline{\hat{t}}_p(a,w;k|l), \tag{8.53}$$

where $p = 1$ or 2 and $l = 0, ..., n$. The "$k+l$ even" notation reminds us of the results expressed in Eq. (8.47).

Equations (8.52) and (8.53) are the desired spectral forms of the surface boundary conditions and are at a notational level equivalent to the radiance transfer equation (8.46).

It should not be overlooked that *when the upper boundary is involved, the amplitude for one l-mode is directly coupled to the amplitudes for all other l-modes.* Thus in Eq. (8.53), $\underline{\hat{L}}_p^+(w;l)$ is determined by sums over k involving $\underline{\hat{L}}_p^-(w;k)$ and $\underline{\hat{L}}_p^+(a;k)$ with $k \neq l$. *This coupling of l-modes is a consequence of the azimuthal anisotropy of the upper boundary.* In

contrast, we recall from the local interaction equations (8.46) that within the isotropic water body (i.e., over the depth range $w \le \zeta \le m$), the amplitude for a given l-mode is independent of the amplitudes for other k-modes, $k \ne l$. This result does *not* negate the computational usefulness of the l-mode decoupling of the radiance amplitudes within the water body $S[w,m]$ because, as we shall see, we can solve for the radiance amplitudes within the water body, independently of the surface boundary conditions.

If the upper boundary were isotropic, symmetry would cause the sums over k in Eqs. (8.52) and (8.53) to collapse to single terms for the lth modes, i.e., the l-modes would decouple. This is the case at the bottom boundary.

Spectral decomposition of the bottom boundary condition ▐▌

The azimuthal isotropy of the bottom boundary implies that the quad-averaged reflectance $r(m,b;r,s{\to}u,v)$ depends at most on $|s-v|$, and not on s and v independently. [For a Lambertian bottom the reflectance is independent of $|s-v|$; see problem 8.3.] We can therefore represent $r(m,b;r,s{\to}u,v)$ by an expansion of the form of Eq. (8.24):

$$r(z,b;r,s{\to}u,v) \;=\; \sum_{l=0}^{n} \hat{r}(z,b;r,u|l)\cos l(\varphi_s - \varphi_v)\,, \tag{8.54}$$

which holds for al Q_{rs} in Ξ_+ and Q_{uv} in Ξ_-. From Eq. (8.25),

$$\hat{r}(z,b;r,u|l) \;=\; \frac{1}{\epsilon_l \cos(l\varphi_s)} \sum_{v=1}^{2n} r(z,b;r,s{\to}u,v)\cos(l\varphi_v)\,. \tag{8.55}$$

As with the phase function, we are free to set $s = 1$ in Eq. (8.55).

We can now apply Eqs. (8.54) and (8.55) to the quad-averaged bottom boundary condition (8.11). We shall leave it as an exercise (problem 8.4) to show that the spectral form of the bottom boundary condition can be written as

$$\hat{\underline{L}}^-_p(m;l) \;=\; \hat{\underline{L}}^+_p(m;l)\,\hat{\underline{r}}_p(m,b;l)\,, \tag{8.56}$$

where $p = 1$ or 2, and $l = 0, ..., n$. Here we have defined the $m{\times}m$ matrix $\hat{\underline{r}}_1(m,b;l)$ by

$$[\hat{\underline{r}}_1(m,b;l)]_{ru} \;\equiv\; \begin{cases} \epsilon_l\,\hat{r}(m,b;r,u|l) & \text{for } r = 1, ..., m-1 \\[4pt] \delta_l\,\hat{r}(m,b;m,u|l) & \text{for } r = m\,, \end{cases} \tag{8.57a}$$

and for u = 1, ..., m and l = 0, ..., n. Matrix $\hat{\underline{r}}_2(m,b;l)$ is defined by

$$
[\hat{\underline{r}}_2(m,b;l)]_{ru} \equiv
\begin{cases}
\gamma_l\, \hat{r}_2(m,b;r,u\,|\,l) & \text{for } r = 1, ..., m{-}1 \\
& \quad\text{and } l = 1, ..., n{-}1\,, \\
0 & \quad\text{for } r = m \\
& \quad\text{or } l = 0 \text{ or } l = n\,,
\end{cases}
\tag{8.57b}
$$

Note that the *l*-modes decouple in Eq. (8.56). For a Lambertian bottom, only the $\hat{\underline{r}}_1(m,b\,|\,0)$ matrix is nonzero, and Eq. (8.56) reduces to just

$$
\hat{\underline{L}}_1^-(m;0) = \hat{\underline{L}}_1^+(m;0)\, \hat{\underline{r}}_1(m,b\,|\,0)\,.
$$

8.6   Fundamental and Transport Solutions for the Radiance Amplitudes

Equations (8.46), (8.52), (8.53), and (8.56) give the spectral forms of the RTE and the boundary conditions. These matrix equations have a mathematical form very similar to the scalar Eqs. (7.1)-(7.5) for the irradiances. Consequently, all of the mathematical constructions based on Eqs. (7.1)-(7.5) – or on their generalizations – can be extended to the spectral matrix equations.

Since the previous chapter discussed invariant imbedding in considerable detail, we shall merely outline the steps in the invariant imbedding solution of the spectral amplitude equations.

Local-transfer-matrix form of the

spectral amplitude equations

The upward and downward local interaction Eqs. (8.46) can be written for each l = 0, 1, ..., *n* as

$$
\frac{d}{d\zeta}\,[\hat{\underline{L}}_p^-(\zeta;l),\ \hat{\underline{L}}_p^+(\zeta;l)] = [\hat{\underline{L}}_p^-(\zeta;l),\ \hat{\underline{L}}_p^+(\zeta;l)]
\begin{bmatrix}
-\hat{\underline{\tau}}(z;l) & \hat{\underline{\rho}}(\zeta;l) \\
& \\
-\hat{\underline{\rho}}(\zeta;l) & \hat{\underline{\tau}}(\zeta;l)
\end{bmatrix}
\tag{8.58}
$$

$$
+\ [-\hat{\underline{S}}_p^-(\zeta;l),\ \hat{\underline{S}}_p^+(\zeta;l)]\,,
$$

or

$$\frac{d}{d\zeta} \hat{\underline{L}}_p(\zeta;l) = \hat{\underline{L}}_p(\zeta;l) \, \underline{K}(\zeta;l) + \hat{\underline{S}}_p(\zeta;l) .$$ (8.59)

Here we have defined the 1×2*m* vectors

$$\hat{\underline{L}}_p(\zeta;l) \equiv [\hat{\underline{L}}_p^-(\zeta;l), \hat{\underline{L}}_p^+(\zeta;l)] ,$$

$$\hat{\underline{S}}_p(\zeta;l) \equiv [-\hat{\underline{S}}_p^-(\zeta;l), \hat{\underline{S}}_p^+(\zeta;l)] ,$$

and the 2*m*×2*m* *spectral local transfer matrix*

$$\underline{K}(\zeta;l) \equiv \begin{bmatrix} -\hat{\underline{t}}(\zeta;l) & \hat{\underline{\rho}}(\zeta;l) \\ -\hat{\underline{\rho}}(\zeta;l) & \hat{\underline{t}}(\zeta;l) \end{bmatrix} .$$ (8.60)

Equation (8.59) is the equivalent of the two-flow Eq. (7.37).

Note that the spectral local transfer matrix $\underline{K}(\zeta;l)$ is independent of *p* = 1, 2. Moreover, the $\underline{K}(\zeta;l)$ of Eq. (8.60) is conceptually simpler than its 2×2 irradiance counterpart $\underline{K}(z)$ seen in Eq. (7.34): *the present* $\underline{K}(\zeta;l)$ *is block antisymmetric and is an inherent optical property*.

We note also that $\underline{K}(\zeta;l)$ is composed of the spectral amplitudes $\hat{\underline{t}}$ and $\hat{\underline{\rho}}$ of the local transmittance and reflectance, whereas $\underline{K}(z)$ was formed from the physical transmittances and reflectances of the irradiances themselves. To be consistent in our notation, we therefore should write $\hat{\underline{K}}(\zeta;l)$. However, no confusion will result if we omit the caret for simplicity, since we never shall need to refer to a radiance $\underline{K}$ composed of physical $\underline{t}$ and $\underline{\rho}$ matrices.

Just as with the two-flow equations, we can generate a *fundamental solution* $\underline{M}(w,\zeta;l)$ *for the spectral amplitudes*. The fundamental solution is now a 2*m*×2*m* matrix for each *l* value. It satisfies

$$\frac{d}{d\zeta} \underline{M}(w,\zeta;l) = \underline{M}(w,\zeta;l) \, \underline{K}(\zeta;l)$$ (8.61)

with the initial conditions

$$\underline{M}(w,w;l) = \underline{I}_{2m} .$$ (8.62)

[Recall Eqs. (7.38) and (7.39).] As with $\underline{K}(\zeta;l)$, we omit the caret from $\underline{M}(w,\zeta;l)$. The same group properties and mapping properties hold for

$\underline{\mathbf{M}}(w,\zeta;l)$ as held for its irradiance counterpart $\underline{\mathbf{M}}(w,z)$. Incorporation of the internal source terms, in parallel to Eqs. (7.41) and (7.42), gives the general solution of Eq. (8.59):

$$\underline{\hat{L}}_p(\zeta;l) = \underline{\hat{L}}_p(w;l)\,\underline{\mathbf{M}}(w,\zeta;l) + \underline{\hat{S}}_p^{\mathbf{f}}(w,\zeta;l) . \qquad (8.63)$$

Here

$$\underline{\hat{S}}_p^{\mathbf{f}}(w,\zeta;l) \equiv \int_w^\zeta \underline{\hat{S}}_p(\zeta';l)\,\underline{\mathbf{M}}(\zeta',\zeta;l)\,d\zeta'$$
$$\equiv \left[\underline{\hat{S}}_p^{-\mathbf{f}}(w,\zeta;l),\ \underline{\hat{S}}_p^{+\mathbf{f}}(w,\zeta;l) \right] . \qquad (8.64)$$

Just as in Eqs. (7.41) and (7.42), the superscript "f" on the fundamental source-induced amplitudes reminds us that they are associated with the fundamental solution via Eq. (8.64).

Transport solution of the spectral amplitude equations

Let us expand Eq. (8.63) to show the upward and downward vectors:

$$\left[\hat{\underline{L}}_p^-(\zeta;l),\ \hat{\underline{L}}_p^+(\zeta;l) \right] = \left[\hat{\underline{L}}_p^-(w;l),\ \hat{\underline{L}}_p^+(w;l) \right]\underline{\mathbf{M}}(w,\zeta;l)$$
$$+ \left[\underline{\hat{S}}_p^{-\mathbf{f}}(w,\zeta;l),\ \underline{\hat{S}}_p^{+\mathbf{f}}(w,\zeta;l) \right] . \qquad (8.65)$$

Now, in parallel to Section 7.6, we note that $\hat{\underline{L}}_p^+(w;\zeta)$ and $\hat{\underline{L}}_p^-(\zeta;l)$ represent the *incident radiances* on the slab $S[w,\zeta]$, and that $\hat{\underline{L}}_p^-(w;l)$ and $\hat{\underline{L}}_p^+(\zeta;l)$ correspond to the *response radiances* leaving $S[w,\zeta]$. Equation (8.65) thus gives the incident and response amplitudes at level ζ, in terms of the incident and response amplitudes at level w. What we need is an equation from which we can obtain both response amplitudes, given the incident amplitudes and the fundamental solution. We can obtain such an equation from clever matrix manipulations of Eq. (8.65).

First, let us rewrite Eq. (8.65) as

$$\left[\hat{\underline{L}}_p^-(\zeta;l),\ \hat{\underline{L}}_p^+(\zeta;l),\ \hat{\underline{L}}_p^-(w;l),\ \hat{\underline{L}}_p^+(w;l) \right]\begin{bmatrix} \underline{I}_{2m} \\ -\underline{\mathbf{M}}(w,\zeta;l) \end{bmatrix}$$
$$= \left[\underline{\hat{S}}_p^{-\mathbf{f}}(w,\zeta;l),\ \underline{\hat{S}}_{-p}^{+\mathbf{f}}(w,\zeta;l) \right] . \qquad (8.66)$$

We wish to rearrange the 1×4m matrix of radiance amplitudes into the order

$$\left[\hat{\underline{L}}^-_p(w;l), \ \hat{\underline{L}}^+_p(\zeta;l), \ \hat{\underline{L}}^-_p(\zeta;l), \ \hat{\underline{L}}^+_p(w;l) \right],$$

so that the first two amplitudes are the response amplitudes and the second two are the incident amplitudes. This can be accomplished by the following matrix mapping:

$$\left[\hat{\underline{L}}^-_p(\zeta;l), \ \hat{\underline{L}}^+_p(\zeta;l), \ \hat{\underline{L}}^-_p(w,l), \ \hat{\underline{L}}^+_b(w,l) \right] \begin{bmatrix} \underline{0} & \underline{0} & \underline{I} & \underline{0} \\ \underline{0} & \underline{I} & \underline{0} & \underline{0} \\ \underline{I} & \underline{0} & \underline{0} & \underline{0} \\ \underline{0} & \underline{0} & \underline{0} & \underline{I} \end{bmatrix}$$

$$= \left[\hat{\underline{L}}^-_p(w;l), \ \hat{\underline{L}}^+_p(\zeta;l), \ \hat{\underline{L}}^-_p(\zeta;l), \ \hat{\underline{L}}^+_p(w;l) \right].$$

Here $\underline{0}$ denotes the m×m matrix of zeros, and $\underline{I}$ is the m×m identity matrix. In addition to accomplishing the desired reordering of the amplitudes, the 4m×4m matrix

$$\underline{P} \equiv \begin{bmatrix} \underline{0} & \underline{0} & \vdots & \underline{I} & \underline{0} \\ \underline{0} & \underline{I} & \vdots & \underline{0} & \underline{0} \\ \cdots & \cdots & \cdots & \cdots & \cdots \\ \underline{I} & \underline{0} & \vdots & \underline{0} & \underline{0} \\ \underline{0} & \underline{0} & \vdots & \underline{0} & \underline{I} \end{bmatrix} \equiv \begin{bmatrix} \underline{P}_2 & \vdots & \underline{P}_1 \\ \cdots & \cdots & \cdots \\ \underline{P}_1 & \vdots & \underline{P}_2 \end{bmatrix} \tag{8.67}$$

has the property that

$$\underline{P}^2 \equiv \underline{P}\,\underline{P} = \underline{I}_{4m}.$$

Therefore, we can insert $\underline{P}^2$ into Eq. (8.66) to get

$$\left[\hat{\underline{L}}^-_p(\zeta;l), \ \hat{\underline{L}}^+_p(\zeta;l), \ \hat{\underline{L}}^-_p(w,l), \ \hat{\underline{L}}^+_p(w;l) \right] \begin{bmatrix} \underline{P}_2 & \underline{P}_1 \\ \underline{P}_1 & \underline{P}_2 \end{bmatrix}^2 \begin{bmatrix} \underline{I}_{2m} \\ -\underline{M}(w,\zeta;l) \end{bmatrix}$$

$$= \left[\hat{\underline{S}}^{-f}_p(w,\zeta;l), \ \hat{\underline{S}}^{+f}_p(w,\zeta;l) \right].$$

The 2m×2m matrices $\underline{P}_1$ and $\underline{P}_2$ are defined by the partitioning of $\underline{P}$ indicated in Eq. (8.67). Operating to the left with one $\underline{P}$ and to the right with the other gives the reordered equation

$$\left[\underline{\hat{L}}_p^-(w;l),\ \underline{\hat{L}}_p^+(\zeta;l),\ \underline{\hat{L}}_p^-(\zeta;l),\ \underline{\hat{L}}_p^+(w;l)\right] \begin{bmatrix} \underline{P}_2 & -\ \underline{P}_1\,\mathbf{M}(w,\zeta;l) \\ \underline{P}_1 & -\ \underline{P}_2\,\mathbf{M}(w,\zeta;l) \end{bmatrix}$$

$$= \left[\ \underline{\hat{S}}_p^{-\,f}(w,\zeta;l),\ \underline{\hat{S}}_p^{+\,f}(w,\zeta;l)\right].$$

Expanding this equation gives

$$\left[\ \underline{\hat{L}}_p^-(w;l),\ \underline{\hat{L}}_p^+(\zeta;l)\right]$$

$$= \left[\ \underline{\hat{L}}_p^-(\zeta;l),\ \underline{\hat{L}}_p^+(w;l)\right]\left[\underline{P}_2\,\mathbf{M}(w,\zeta;l) - \underline{P}_1\right]\left[\underline{P}_2 - \underline{P}_1\,\mathbf{M}(w,\zeta;l)\right]^{-1} \quad (8.68)$$

$$+ \left[\ \underline{\hat{S}}_p^{-\,f}(w,\zeta;l),\ \underline{\hat{S}}_p^{+\,f}(w,\zeta;l)\right]\left[\underline{P}_2 - \underline{P}_1\,\mathbf{M}(w,\zeta;l)\right]^{-1}.$$

This equation now gives the response amplitudes in terms of the incident amplitudes, the fundamental solution, and other known quantities. The continuity of $\underline{K}(\zeta;l)$ in Eq. (8.61) guarantees the existence of the inverse matrices in Eq. (8.68).

If we partition $\mathbf{M}(w,\zeta;l)$ into $m \times m$ blocks of the form

$$\mathbf{M}(w,\zeta;l) \equiv \begin{bmatrix} \mathbf{M}_{--}(w,\zeta;l) & \mathbf{M}_{-+}(w,\zeta;l) \\ \mathbf{M}_{+-}(w,\zeta;l) & \mathbf{M}_{++}(w,\zeta;l) \end{bmatrix} \quad (8.69)$$

and substitute for $\underline{P}_1$ and $\underline{P}_2$ from Eq. (8.67), it is easy to show that Eq. (8.68) has precisely the form of Eqs. (7.49) and (7.50). We are thus led to the spectral amplitude equivalent of Eqs. (7.47) and (7.48):

$$\left[\ \underline{\hat{L}}_p^-(w;l),\ \underline{\hat{L}}_p^+(\zeta;l)\right] = \left[\ \underline{\hat{L}}_p^-(\zeta;l),\ \underline{\hat{L}}_p^+(w;l)\right]\begin{bmatrix} \underline{T}(\zeta,w;l) & \underline{R}(\zeta,w;l) \\ \underline{R}(w,\zeta;l) & \underline{T}(w,\zeta;l) \end{bmatrix}$$

$$+ \left[\hat{S}_p^{-\,t}(\zeta,w;l),\ \hat{S}_p^{+\,t}(w,\zeta;l)\right]. \quad (8.70)$$

Here the $\underline{T}$'s and $\underline{R}$'s are the $m \times m$ *spectral standard transmittance* and *spectral standard reflectance matrices for the slab* $S[w,\zeta]$. The internal-source terms $[\hat{S}_p^{-\,t}(\zeta,w;l),\ \hat{S}_p^{+\,t}(w,\zeta;l)]$ are defined analogously to $[E_u^t(z,w),\ E_d^t(w,z)]$ in Eq. (7.52), as can be seen by expanding the last term in Eq. (8.68). We have added the superscript "t" to the $\hat{S}_p^{\pm\,t}$ terms to remind us of the close parallel with E_u^t and E_d^t.

Equations (8.70) are the *spectral downward global interaction principles for slab S[w,ζ]*. In exact analogy with the two-flow irradiance Eqs. (7.55) and (7.56), we have the *spectral upward global interaction principles for the slab S[ζ,m]*:

$$\left[\underline{\hat{L}}_p^-(\zeta;l), \ \underline{\hat{L}}_p^+(m;l) \right] = \left[\underline{\hat{L}}_p^-(m;l), \ \underline{\hat{L}}_p^+(\zeta;l) \right] \begin{bmatrix} \underline{T}(m,\zeta;l) & \underline{R}(m,\zeta;l) \\ \underline{R}(\zeta,m;l) & \underline{T}(\zeta,m;l) \end{bmatrix}$$

$$+ \left[\hat{S}_p^{-t}(m,\zeta;l), \ \hat{S}_p^{+t}(\zeta,m;l) \right]. \tag{8.71}$$

Equations (8.70) and (8.71) constitute the *transport solution for the spectral radiance amplitudes* within the water body *S[w,m]*.

The $\underline{T}$'s and $\underline{R}$'s in Eqs. (8.70) and (8.71) connect radiance amplitudes, rather than physical radiances. These $\underline{T}$'s and $\underline{R}$'s therefore should be written with carets for consistency of notation. However, as with $\underline{K}$ and $\underline{M}$, we omit the carets for simplicity.

Note that setting $\zeta = w$ in Eq. (8.70) gives

$$\underline{T}(w,w;l) = \underline{I}_m$$

$$\underline{R}(w,w;l) = \underline{0}_m \tag{8.72}$$

$$\left[\underline{\hat{S}}_p^{-t}(w,w;l), \ \underline{\hat{S}}_p^{+t}(w,w;l) \right] = \left[\underline{0}_{1\times m}, \ \underline{0}_{1\times m} \right].$$

These initial conditions correspond to Eqs. (7.53) and (7.54). A corresponding set of conditions,

$$\underline{T}(m,m;l) = \underline{I}_m$$

$$\underline{R}(m,m;l) = \underline{0}_m \tag{8.73}$$

$$\left[\underline{\hat{S}}_p^{-t}(m,m;l), \ \underline{\hat{S}}_p^{+t}(m,m;l) \right] = \left[\underline{0}_{1\times m}, \ \underline{0}_{1\times m} \right],$$

is obtained from Eq. (8.71) by setting $\zeta = m$; recall Eqs. (7.59) and (7.60). Finally, note that the spectral standard operators depend on the *l*-mode, but not on $p = 1, 2$ or on the upward/downward index.

We can obtain the spectral standard transmittances and reflectances from the fundamental solution matrix $\mathbf{M}(w,\zeta;l)$, which is obtained by integrating Eq. (8.61) downward from w to ζ, starting with initial condition (8.62). The connection between the fundamental solution and the standard

matrices is easily obtained by expanding Eq. (8.68), using Eqs. (8.67) and (8.69), and comparing the result with Eq. (8.70). The transport source terms are obtained in a similar fashion from Eqs. (8.64), (8.68), and (8.70). These connections have exactly the same form as Eqs. (7.51) and (7.52).

However, the computationally most efficient path to the needed quantities is via Riccati equations.

8.7   Differential Equations for the Standard Operators

We can derive downward and upward sextets of Riccati equations for the matrix spectral standard operators, exactly as was done for the scalar operators in Section 7.8. For example, we can expand the downward global interaction Eqs. (8.70) to get two matrix equations. We then differentiate the equation involving $\underline{\hat{L}}_p^+(\zeta;l)$, and use the local interaction Eqs. (8.46) to replace the ζ-derivative of the amplitudes. Grouping terms as in Eq. (7.113) and repeating the arguments about the arbitrariness of the incident amplitudes and internal sources yields the major downward trio of matrix Riccati equations corresponding to Eqs. (7.114)-(7.116). The other three triplets of equations follow in the same fashion. In these deviations, it is of course necessary to pay careful attention of the order of the matrices, since matrix multiplication does not commute, in general.

Without further ado, we display *the Riccati differential equations for the standard operators for the radiance amplitudes*. The downward sextet, derived from the downward global interaction principles (8.70), is

$$\frac{d}{d\zeta}\,\underline{R}(\zeta,w;l) \;=\; \underline{R}(\zeta,w;l)\left[\underline{\hat{t}}(\zeta;l)\;+\;\underline{\hat{\rho}}(\zeta;l)\,\underline{R}(\zeta,w;l)\,\right]$$
$$+\;\underline{\hat{\rho}}(\zeta;l)\;+\;\underline{\hat{t}}(\zeta;l)\,\underline{R}(\zeta,w;l) \tag{8.74}$$

$$\frac{d}{d\zeta}\,\underline{T}(w,\zeta;l) \;=\; \underline{T}(w,\zeta;l)\left[\underline{\hat{t}}(\zeta;l)\;+\;\underline{\hat{\rho}}(\zeta;l)\,\underline{R}(\zeta,w;l)\,\right] \tag{8.75}$$

$$\frac{d}{d\zeta}\,\underline{T}(\zeta,w;l) \;=\; \left[\,\underline{\hat{t}}(\zeta;l)\;+\;\underline{R}(\zeta,w;l)\,\underline{\hat{\rho}}(\zeta;l)\,\right]\underline{T}(\zeta,w;l) \tag{8.76}$$

$$\frac{d}{d\zeta}\,\underline{R}(w,\zeta;l) \;=\; \underline{T}(w,\zeta;l)\,\underline{\hat{\rho}}(\zeta;l)\,\underline{T}(\zeta,w;l) \tag{8.77}$$

$$\frac{d}{d\zeta}\,\underline{\hat{S}}_p^{+t}(w,\zeta;l) \;=\; \underline{\hat{S}}_p^{+t}(w,\zeta;l)\left[\,\hat{\underline{t}}(\zeta;l) \;+\; \hat{\underline{\rho}}(\zeta;l)\,\underline{R}(\zeta,w;l)\,\right]$$

$$+\; \underline{\hat{S}}_p^{+}(\zeta;l) \;+\; \underline{\hat{S}}_p^{-}(\zeta;l)\,\underline{R}(\zeta,w;l) \tag{8.78}$$

$$\frac{d}{d\zeta}\underline{\hat{S}}_p^{-t}(\zeta,w;l) \;=\; \left[\,\underline{\hat{S}}_p^{-}(\zeta;l) \;+\; \underline{\hat{S}}_p^{+t}(w,\zeta;l)\,\hat{\underline{\rho}}(\zeta;l)\,\right]\underline{T}(\zeta,w;l) \tag{8.79}$$

The forms of these matrix equations should be compared to the scalar equations for the irradiance transmittances and reflectances, Eqs. (7.114)-(7.119),

The upward sextet, derived from the upward global interaction principles (8.71), is

$$-\frac{d}{d\zeta}\,\underline{R}(\zeta,m;l) \;=\; \underline{R}(\zeta,m;l)\left[\,\hat{\underline{t}}(\zeta;l) \;+\; \hat{\underline{\rho}}(\zeta;l)\,\underline{R}(\zeta,m;l)\,\right]$$

$$+\; \hat{\underline{\rho}}(\zeta;l) \;+\; \hat{\underline{t}}(\zeta;l)\,\underline{R}(\zeta,m;l) \tag{8.80}$$

$$-\frac{d}{d\zeta}\,\underline{T}(m,\zeta;l) \;=\; \underline{T}(m,\zeta;l)\left[\,\hat{\underline{t}}(\zeta;l) \;+\; \hat{\underline{\rho}}(\zeta;l)\,\underline{R}(\zeta,m;l)\,\right] \tag{8.81}$$

$$-\frac{d}{d\zeta}\,\underline{T}(\zeta,m;l) \;=\; \left[\,\hat{\underline{t}}(\zeta;l) \;+\; \underline{R}(\zeta,m;l)\,\hat{\underline{\rho}}(\zeta;l)\,\right]\underline{T}(\zeta,m;l) \tag{8.82}$$

$$-\frac{d}{d\zeta}\,\underline{R}(m,\zeta;l) \;=\; \underline{T}(m,\zeta;l)\,\hat{\underline{\rho}}(\zeta;l)\,\underline{T}(\zeta,m;l) \tag{8.83}$$

$$-\frac{d}{d\zeta}\,\underline{\hat{S}}_p^{-t}(m,\zeta;l) \;=\; \underline{\hat{S}}_p^{-t}(m,\zeta;l)\left[\,\hat{\underline{t}}(\zeta;l) \;+\; \hat{\underline{\rho}}(\zeta;l)\,\underline{R}(\zeta,m;l)\,\right]$$

$$+\; \underline{\hat{S}}_p^{-}(\zeta;l) \;+\; \underline{\hat{S}}_p^{+}(\zeta;l)\,\underline{R}(\zeta,m;l) \tag{8.84}$$

$$-\frac{d}{d\zeta}\,\underline{\hat{S}}_p^{+t}(\zeta,m;l) \;=\; \left[\,\underline{\hat{S}}_p^{+}(\zeta;l) \;+\; \underline{\hat{S}}_p^{-t}(m,z;l)\,\hat{\underline{\rho}}(\zeta;l)\,\right]\underline{T}(\zeta,m;l) \tag{8.85}$$

These equations correspond to Eqs. (7.121)-(7.126).

In Eqs. (8.74)-(8.85), all quantities are $m{\times}m$ matrices, except for the $\underline{\hat{S}}$'s, which are $1{\times}m$ matrices. An independent set of equations is obtained for each value of $l = 0$, 1, ..., n, and for each value of $p = 1$, 2 in the internal-source equations. For a typical value of m, say 10 or 15, we thus have a thousand or more coupled differential equations, which must be

integrated *n*+1 times to account for each *l* value. The numerical integration of such systems of equations can be carried out with great accuracy and efficiency using, for example, a high-order Runge-Kutta algorithm. Most libraries of mathematical software have routines designed for just such systems of equations.

The integration of these equations proceeds slightly differently from that of the corresponding irradiance-level equations. In particular, in Section 7.8 we incorporated the surface boundary conditions into the solutions of the Riccati equations by integrating Eqs. (7.114)-(7.119) with initial conditions (7.120), and by integrating Eqs (7.121)-(7.126) with initial conditions (7.127). However, as we already have seen, the *l*-modes do not decouple in the present surface boundary conditions. Thus we cannot solve Eqs. (8.74)-(8.85) one *l*-mode at a time and also simultaneously incorporate the surface boundary conditions. We therefore must integrate Eqs. (8.74)-(8.85) with boundary conditions describing a bare slab $S[w,\zeta]$, and then incorporate the boundary effects of slab $S[a,w]$ at a later time. These bare-slab initial conditions are given by Eqs. (8.72) for the downward Riccati sextet, and by Eqs. (8.73) for the upward sextet. Recall the parenthetical bare-slab initial conditions shown in Eqs. (7.120) and (7.127).

Indeed, *one of the great virtues of the present formulation is that it allows us to solve the radiance transfer problem within the water body itself, without any consideration whatsoever of the surface and bottom boundary conditions to be imposed on the water body S[w,m].* By postponing the incorporation of the boundary effects until the last moment, we can couple different boundary conditions with the same interior solution, and thereby obtain a set of different total solutions with a minimum of computation. Conversely, we can compute and save once and for all a set of spectral surface transfer functions $\hat{t}_p(a,x;k|l)$, etc., which correspond to a given wind speed and quad partitioning. We can then use these surface transfer functions repeatedly as we change the IOP's of the water body. We need only re-integrate the Riccati equations for each new set of IOP's, and then recall and incorporate the stored boundary conditions. This separation of the computations related to the boundaries $S[a,w]$ and $S[m,b]$, and to the interior $S[w,m]$, results in enormous computational savings in systematic studies requiring the solution of the RTE for many different boundary and interior conditions. Such a partitioning of the computations is inherently impossible in Monte Carlo simulations.

8.8   Composite Forms of the *l*-mode Equations

In order to complete the solution of the RTE, we must couple the boundary conditions with the interior solution just obtained in the form of the standard operators and transport source terms. This coupling is most easily accomplished if we write our equations in a compact form that combines all *l*-modes.

The surface boundary conditions (8.52) and (8.53) explicitly show the $m \times m$ transfer matrices $\hat{\underline{t}}_p(a,w;k|l)$, etc., and the $1 \times m$ amplitude matrices $\hat{\underline{L}}_p(a;l)$, etc. In these equations k and l run from 0 to n, but the transfer matrices are nonzero only when $k+l$ is even. Now let us define an $m(n+1) \times m(n+1)$ block matrix $\hat{\underline{t}}_p(a,w)$ using the $n+1$ different $m \times m$ $\hat{\underline{t}}_p(a,w;k|l)$ matrices:

$$\hat{\underline{t}}_p(a,w) \equiv$$

$$\begin{bmatrix} \hat{\underline{t}}_p(a,w;0|0) & \underline{0} & \hat{\underline{t}}_p(a,w;0|2) & \underline{0} & \cdots & \hat{\underline{t}}_p(a,w;0|n) \\ \underline{0} & \hat{\underline{t}}_p(a,w;1|1) & \underline{0} & \hat{\underline{t}}_p(a,w;1|3) & \cdots & \underline{0} \\ \hat{\underline{t}}_p(a,w;2|0) & \underline{0} & \hat{\underline{t}}_p(a,w;2|2) & \underline{0} & \cdots & \hat{\underline{t}}_p(a,w;2,n) \\ \vdots & \vdots & \vdots & \vdots & \vdots & \vdots \\ \hat{\underline{t}}_p(a,w;n|0) & \underline{0} & \hat{\underline{t}}_p(a,w;n|2) & \underline{0} & \cdots & \hat{\underline{t}}_p(a,w;n|n) \end{bmatrix} \tag{8.86}$$

Here $\underline{0}$ is the $m \times m$ matrix of zeros. The checkerboard pattern results from requirement that $k+l$ be even. Similar definitions are made for the other three transfer functions. Let us also combine the *l*-mode radiance amplitudes $\hat{\underline{L}}_p^-(a;l)$ into one $1 \times m(n+1)$ matrix:

$$\hat{\underline{L}}_p^-(a) \equiv \left[\hat{\underline{L}}_p^-(a;0),\ \hat{\underline{L}}_p^-(a;1),...,\ \hat{\underline{L}}_p^-(a;n) \right], \tag{8.87}$$

with corresponding definitions for the other amplitudes.

Using matrices of the forms shown in Eqs. (8.86) and (8.87), the air-water surface boundary condition (8.52) can be written as

$$\hat{\underline{L}}_p^-(a) = \hat{\underline{L}}_p^-(w)\, \hat{\underline{t}}_p(w,a)\ +\ \hat{\underline{L}}_p^+(a)\, \hat{\underline{r}}_p(a,w), \tag{8.88}$$

and Eq. (8.53) becomes

$$\hat{\underline{L}}_p^+(w) = \hat{\underline{L}}_p^-(w)\,\hat{\underline{r}}_p(w,a) + \hat{\underline{L}}_p^+(a)\,\hat{\underline{t}}_p(a,w)\,. \tag{8.89}$$

The global interaction Eqs. (8.70) also can be written in a form that combines all *l*-modes. To do this, we first combine each of the spectral standard transmittance and reflectance matrices for the different *l*-modes into one $m(n+1)\times m(n+1)$ matrix, e.g.

$$\underline{T}(\zeta,w) \equiv \begin{bmatrix} \underline{T}(\zeta;w;0) & \underline{0} & \underline{0} & \cdots & \underline{0} \\ \underline{0} & \underline{T}(\zeta,w;1) & \underline{0} & \cdots & \underline{0} \\ \vdots & & \ddots & & \vdots \\ \underline{0} & & \cdots & & \underline{T}(\zeta,w;n) \end{bmatrix}. \tag{8.90}$$

Using these matrices along with those of Eq. (8.87), the two equations contained within Eq. (8.70) can be written as

$$\hat{\underline{L}}_p^-(w) = \hat{\underline{L}}_p^-(\zeta)\,\underline{T}(\zeta,w) + \hat{\underline{L}}_p^+(w)\,\underline{R}(w,\zeta) + \hat{\underline{S}}_p^{-t}(\zeta,w) \tag{8.91}$$

$$\hat{\underline{L}}_p^+(\zeta) = \hat{\underline{L}}_p^-(\zeta)\,\underline{R}(\zeta,w) + \hat{\underline{L}}_p^+(w)\,\underline{T}(w,\zeta) + \hat{\underline{S}}_p^{+t}(w,\zeta)\,. \tag{8.92}$$

Finally, the bottom boundary condition (8.56) can be written

$$\hat{\underline{L}}_p^-(m) = \hat{\underline{L}}_p^+(m)\,\hat{\underline{r}}_p(m,b)\,, \tag{8.93}$$

where $\hat{\underline{r}}_p(m,b)$ is a block diagonal matrix of the form (8.90).

In each of the Eqs. (8.88)-(8.93), independent sets of equations are obtained for the cosine and sine amplitudes, i.e., for $p = 1$ and 2. Note that each of the Eqs. (8.88)-(8.89) and (8.91)-(8.93) have the form of global interaction equations for the appropriate slabs. The forms of these equations should be compared with their scalar counterparts. For example, compare Eq. (8.88) with Eq. (7.1), and compare Eq. (8.91) with Eq. (7.47).

8.9   Completing the Solution

The remaining steps in the solution of the RTE are straightforward. We need only elevate the various scalar formulas developed for the two-flow solution into matrix formulas applicable to the present problem.

Integrating the Riccati equations

Let us assume that we wish to compute the radiance distribution at a finite set of optical depths ζ_k, $k = 1, 2, ..., K$, within the water body $S[w,m]$, where $w \equiv \zeta_1 < \zeta_2 < ... < \zeta_K \equiv m$. In general, we first integrate the Riccati Eqs. (8.74)-(8.79) in a downward sweep from depth w to depth m, starting with initial conditions (8.72). Each l value is a separate integration. Save the results at each depth of interest, i.e., store the matrices $\underline{R}(\zeta_1,w;l)$ $(= \underline{I})$, $\underline{R}(\zeta_2,w;l)$, ..., $\underline{R}(m,w;l)$, and so on, for each $l = 0, ..., n$.

Because we have restricted the bottom boundary $S[m,b]$ to be a reflecting slab without light transmission from below, we will not need $\underline{R}(w,\zeta;l)$. $\underline{T}(\zeta,w;l)$ is needed only in the source-term Eq. (8.79). Thus if we are modeling a source-free water body, only Eqs. (8.74) and (8.75) need to be integrated, in order to obtain $\underline{R}(\zeta,w;l)$ and $\underline{T}(w,\zeta;l)$.

Next integrate Eqs. (8.80)-(8.85) in an upward sweep from m to w, starting with the general initial condition (8.73), and save the results at each depth of interest. For source-free water with an opaque reflecting bottom, only $\underline{R}(\zeta,m;l)$ needs to be computed by integration of Eq. (8.80). If internal sources are present, $\underline{T}(\zeta,m;l)$ must also be computed along with the source terms, as seen in Eq. (8.85).

For an isotropic bottom boundary, which we are now considering, we can incorporate the bottom boundary effects into the computed $\underline{R}(\zeta,m;l)$ for each l value. This is because the bottom boundary condition decouples for each l-mode; recall Eq. (8.56). The most computationally efficient process is then to integrate Eq. (8.80) twice, once for $p = 1$ and once for $p = 2$, in order to generate the two matrices $\underline{R}_1(\zeta,b;l)$ and $\underline{R}_2(\zeta,b;l)$. The initial conditions for these two integrations are, respectively,

$$\underline{R}_1(m,b;l) = \hat{\underline{r}}_1(m,b;l)$$
$$\underline{R}_2(m,b;l) = \hat{\underline{r}}_2(m,b;l) ,$$

(8.94)

where the $\hat{\underline{r}}_p(m,b;l)$ describe either a Lambertian or an infinitely deep bottom. Note that we have now changed the second argument of $\underline{R}(\zeta,m;l)$ from m to b to indicate that the bottom effects are already incorporated into $\underline{R}_b$.

Integration of the Riccati equations requires that $\hat{\tau}(\zeta;l)$ and $\hat{\rho}(\zeta;l)$ be continuous functions of depth. For homogeneous water bodies, these quantities are independent of depth. If the water is inhomogeneous and the IOP's are given as continuous analytic functions of depth, we can compute $\hat{\tau}(\zeta;l)$ and $\hat{\rho}(\zeta;l)$ at each depth as we integrate. It more often occurs that we are given a set of IOP's measured at discrete geometric depths z_i, $i = 1, ..., I$.

In this case, we can fit a continuous function to the given IOP's (e.g., a piecewise linear function between the given z_i, or perhaps a spline function), and we can determine the optical depth corresponding to a given geometric depth z by integration of Eq. (4.2). It is computationally expedient (and almost always satisfactory) to compute values for $\hat{\tau}(\zeta_i;l)$ and $\hat{\rho}(\zeta_i;l)$ at the ζ_i values corresponding to the z_i, and then to use linear interpolation to obtain $\hat{\tau}(\zeta;l)$ and $\hat{\rho}(\zeta;l)$ at all other ζ values needed in the course of integration of the Riccati equations.

After integrating the Riccati equations, we know $\underline{R}(\zeta_k,w;l)$, $\underline{T}(w,\zeta_k;l)$, $\underline{R}_1(\zeta_k,b;l)$, $\underline{R}_2(\zeta_k,b;l)$ and, if present, the internal source terms $\hat{\underline{S}}_p^{+t}(w,\zeta_k;l)$, etc. Note that *these quantities define the radiative transfer properties of the "bare" water body S[w,m] plus the bottom boundary S[m,b]*. In order to compute the radiance amplitudes themselves, we must incorporate the effects of the incident sky radiance and the transport properties of the air-water surface.

Incorporation of the air-water surface boundary conditions

In exact analogy to Eq. (7.98), we can write an invariant imbedding rule for depths (a,w,b):

$$\hat{\underline{L}}_p^+(w) = \hat{\underline{L}}_p^-(b)\,\mathbf{R}_p(b,w,a) \;+\; \hat{\underline{L}}_p^+(a)\,\mathbf{T}_p(a,w,b) \;+\; \mathbf{S}_p(a,w,b)\,. \qquad (8.95)$$

Let us first note that $\hat{\underline{L}}_p^-(b) = \underline{0}$, because we are assuming that there is no radiance incident upward from below the bottom boundary. The remaining *spectral complete operators* $\mathbf{T}$ and $\mathbf{S}$ are now $m(n+1){\times}m(n+1)$ matrices, which of necessity incorporate all l-modes. Note that these quantities depend on p = 1, 2 because the boundary transfer functions and internal source terms differ for the cosine and sine amplitudes. These operators can be expressed in terms of the composite standard operators by equations of the form of Eqs. (7.102) and (7.104):

$$\mathbf{T}_p(a,w,b) \equiv \hat{\underline{t}}_p(a,w)\Big[\underline{I} - \underline{R}_p(w,b)\,\hat{\underline{r}}_p(w,a)\Big]^{-1} \qquad (8.96)$$

$$\mathbf{S}_p(a,w,b) \equiv \Big[\hat{\underline{S}}_p^{+t}(a,w) + \hat{\underline{S}}_p^{-t}(b,w)\,\hat{\underline{r}}_p(w,a)\Big]\Big[\underline{I} - \underline{R}_p(w,b)\,\hat{\underline{r}}_p(w,a)\Big]^{-1} \quad (8.97)$$

In Eq. (8.97), $\hat{\underline{S}}_p^{+t}(a,w) = \underline{0}$ because we are assuming the air-water surface to be source-free. The $\hat{\underline{t}}_p(a,w)$, $\underline{R}_p(w,b)$, etc are all $m(n+1){\times}m(n+1)$ matrices, defined as in Eqs. (8.86) and (8.90).

Except for $\underline{\hat{L}}_p^+(w)$, all of the quantities in Eqs. (8.95)-(8.97) are known either from the surface boundary conditions or from the Riccati equations. The remaining parts of Eqs. (8.95)-(8.97) can be combined to give

$$\underline{\hat{L}}_p^+(w) = \left[\underline{\hat{L}}_p^+(a)\, \hat{\underline{t}}_p(a,w) + \hat{\underline{S}}_p^{-t}(b,w)\, \hat{\underline{r}}_p(w,a) \right] \left[\underline{I} - \underline{R}_p(w,b)\, \hat{\underline{r}}_p(w,a) \right]^{-1} \quad (8.98)$$

All of the quantities in the right-hand-side of Eq. (8.98) are known either from the surface boundary conditions or from the Riccati equations. We therefore now use Eq. (8.98) to compute $\underline{\hat{L}}_p^+(w)$.

It is worth a moment's pause to review the physical interpretation of Eq. (8.98). The first term in square brackets represents (in spectral form) the incident sky radiance transmitted downward through the air-water surface. The second term represents the upward radiance at level w generated by the internal sources throughout the water body; this upward radiance is then reflected back downward by the air-water surface. These two contributions to the downward radiance at w then undergo an infinite series of inter-reflections between the water body plus bottom, $S[w,b]$, and the surface $S[a,w]$, as described in the discussion of Eq. (7.19) and in Fig. 7.1.

We also should point out the difference between Eqs. (8.98) and (8.89). Both equations give $\underline{\hat{L}}_p^+(w)$, but in much different forms. Boundary condition (8.89) gives $\underline{\hat{L}}_p^+(w)$ in terms of the incident amplitudes $\underline{L}_p^+(a)$ and the upwelling amplitudes $\underline{L}_p^-(w)$, *which we do not yet know*. Equation (8.98), on the other hand, gives $\underline{\hat{L}}_p^+(w)$ in terms of $\underline{\hat{L}}_p^+(a)$ and other *known* quantities. Both equations are of course true, but only Eq. (8.98) is useful at this stage of our calculations.

The invariant imbedding rule for depths (a,w,b) corresponding to Eq. (7.97) is

$$\underline{\hat{L}}_p^-(w) = \underline{\hat{L}}_p^-(b)\, \underline{T}_p(b,w,a) + \underline{\hat{L}}_p^+(a)\, \underline{R}_p(a,w,b) + \underline{S}_p(b,w,a). \qquad (8.99)$$

As already noted, $\underline{\hat{L}}_p^-(b) = \underline{0}$, and $\underline{R}(a,w,b)$ and $\underline{S}_p(b,w,a)$ are given by the equivalents of Eqs. (7.103) and (7.101), respectively:

$$\underline{R}_p(a,w,b) \equiv \hat{\underline{t}}_p(a,w) \left[\underline{I} - \underline{R}_p(w,b)\, \hat{\underline{r}}_p(w,a) \right]^{-1} \underline{R}_p(w,b) \qquad (8.100)$$

$$\underline{S}_p(b,w,a) \equiv \left[\hat{\underline{S}}_p^{-t}(b,w) + \hat{\underline{S}}_p^{+t}(a,w)\, \underline{R}_p(w,b) \right] \left[\underline{I} - \hat{\underline{r}}_p(w,a)\, \underline{R}_p(w,b) \right]^{-1} (8.101)$$

As already noted, $\hat{S}_p^{+t}(a,w) = \underline{0}$. Equations (8.99)-(8.101) thus reduce to

$$
\begin{aligned}
\hat{\underline{L}}_p^-(w) &= \hat{\underline{L}}_p^+(a)\,\hat{\underline{t}}_p(a,w)\left[\underline{I} - \underline{R}_p(w,b)\,\hat{\underline{r}}_p(w,a)\right]^{-1}\underline{R}_p(w,b) \\
&\quad + \hat{\underline{S}}_p^{-t}(b,w)\left[\underline{I} - \hat{\underline{r}}_p(w,a)\,\underline{R}_p(w,b)\right]^{-1}.
\end{aligned}
\tag{8.102}
$$

All of the terms on the right-hand side of (8.102) are now known, and so we can determine $\hat{L}_p^-(w)$. The physical interpretation of Eq. (8.102) is analogous to that for Eq. (8.98).

We now know the radiance amplitudes just below the air-water surface, including all effects of the incident sky radiance, the internal sources, the surface and bottom boundaries, and the water body itself.

We next compute the radiance amplitudes throughout the water body.

Interior radiance amplitudes

Invariant imbedding rules for depths (w,ζ_k,b) can be written for each l value, since the l-modes decouple within the water body. In general, these equations are

$$
\begin{aligned}
\hat{\underline{L}}_p^+(\zeta_k;l) &= \hat{\underline{L}}_p^-(b;l)\,\underline{\mathbf{R}}_p(b,\zeta_k,w;l) \\
&\quad + \hat{\underline{L}}_p^+(w;l)\,\underline{\mathbf{T}}_p(w,\zeta_k,b;l) + \underline{\mathbf{S}}_p(w,\zeta_k,b;l)
\end{aligned}
\tag{8.103}
$$

and

$$
\begin{aligned}
\hat{\underline{L}}_p^-(\zeta_k;l) &= \hat{\underline{L}}_p^-(b;l)\,\underline{\mathbf{T}}_p(b,\zeta_k,w;l) \\
&\quad + \hat{\underline{L}}_p^+(w;l)\,\underline{\mathbf{R}}_p(w,\zeta_k,b;l) + \underline{\mathbf{S}}_p(b,\zeta_k,w;l).
\end{aligned}
\tag{8.104}
$$

The matrices in Eqs. (8.103) and (8.104) are now $m{\times}m$ or $1{\times}m$, since we have decomposed our equations into $n{+}1$ separate sets of equations for $l = 0, 1, ..., n$. As before, $\hat{\underline{L}}_p^-(b;l) = \underline{0}$. We leave it to the reader to show that Eqs. (8.103) and (8.104) can be written as

$$
\begin{aligned}
\hat{\underline{L}}_p^+(\zeta_k;l) &= \hat{\underline{L}}_p^+(w;l)\,\underline{T}(w,\zeta_k;l)\left[\underline{I} - \underline{R}_p(\zeta_k,b;l)\,\underline{R}(\zeta_k,w;l)\right]^{-1} \\
&\quad + \left[\hat{\underline{S}}_p^{+t}(w,\zeta_k;l) + \hat{\underline{S}}_p^{-t}(b,\zeta_k;l)\,\underline{R}(\zeta_k,w;l)\right]\left[\underline{I} - \underline{R}_p(\zeta_k,b;l)\,\underline{R}(\zeta_k,w;l)\right]^{-1}
\end{aligned}
\tag{8.105}
$$

and

$$\hat{\underline{L}}_p^-(\zeta_k;l) = \hat{\underline{L}}_p^+(w;l)\,\underline{T}(w,\zeta_k;l)\left[\,\underline{I} - \underline{R}_p(\zeta_k,b;l)\,\underline{R}(\zeta_k,w;l)\,\right]^{-1}\underline{R}_p(\zeta_k;b;l)$$

$$+\left[\,\hat{\underline{S}}_p^{-t}(b,\zeta_k;l) + \hat{\underline{S}}_p^{+t}(w,\zeta_k;l)\,\underline{R}_p(\zeta_k,b;l)\,\right]\left[\,\underline{I} - \underline{R}(\zeta_k,w;l)\,\underline{R}_p(\zeta_k,b;l)\,\right]^{-1} . \tag{8.106}$$

All of the quantities on the right-hand sides of these equations are known, either from Eqs. (8.98) and (8.102) or from the results of the Riccati integrations saved at depths ζ_k. We therefore can use Eqs. (8.105) and (8.106) to compute the radiance amplitudes at all depths ζ_k, $k = 2, ..., K$ (recall that $\zeta_1 \equiv w$) for all l and p values.

Water-leaving radiance amplitudes

The only quantity still unknown is $\hat{\underline{L}}_p^-(a)$, the spectral amplitude for the upward radiance just above the air-water surface. This quantity can be obtained from the surface boundary condition (8.88):

$$\hat{\underline{L}}_p^-(a) = \hat{\underline{L}}_p^-(w)\,\hat{\underline{t}}_p(w,a) + \hat{\underline{L}}_p^+(a)\,\hat{\underline{r}}_p(a,w) . \tag{8.107}$$

This computation must be performed simultaneously for all l-modes.

Synthesis of the quad-averaged radiances

We have now computed the radiance amplitudes

$$\hat{\underline{L}}_p^\pm(\zeta;l) = \left[\,\hat{L}_p^\pm(\zeta;1;l), ..., \hat{L}_p^\pm(\zeta;m;l)\,\right]$$

for every depth $a \leq w \leq \zeta_k \leq m$, and for each p and l value. The final step in the solution of the RTE is to return to Eq. (8.31) and compute the quad-averaged radiances from these spectral amplitudes. We thus apply

$$L^\pm(\zeta;u,v) = \sum_{l=0}^n \left[\,\hat{L}_1^\pm(\zeta;u;l)\cos(l\phi_v) + \hat{L}_2^\pm(\zeta;u;l)\sin(l\phi_v)\,\right] \tag{8.108}$$

at each depth a, $w = \zeta_1, \zeta_2, ..., \zeta_K = m$, and for each value of $u = 1, ..., m$ and $v = 1, ..., 2n$, in order to obtain the desired quad-averaged radiances (but note that when $u = m$, the special case for polar caps as seen in the first line of Eq. 8.32 must be used). *This step completes the numerical solution of the radiance transfer equation.* Hallelujah!

8.10 Summary

We now have developed in detail an algorithm for solving the RTE (5.24). The relevant equations are spread over many pages; a compact, graphical summary of the solution steps is therefore of value. Figure 8.1 shows the initial calculations in flowchart format. The direction of the arrows shows the logical dependency of these calculations. Note, for example, that the calculations related to the air-water surface depend on the choice of quad-partitioning and wind speed, but are independent of all else. Likewise, the phase function calculations depend only on the quad partitioning and the choice of the phase functions. The computations of the spectral amplitudes for the surface transfer functions and for the phase functions require much of the computer time for the complete solution. However, these are one-time calculations, whose stored results can be used repeatedly (at almost no computer expense) for different choices of the remaining problem parameters: sky radiance, IOP's, bottom boundary condition, and so on.

After the problem has been defined and initial calculations have been performed, we proceed with the solution as shown in Fig. 8.2. The integration of the Riccati equations is the other main consumer of computer time. These computations must be repeated any time the IOP's, internal sources, output depths or bottom boundary conditions are changed. In other words, the Riccati equations must be integrated for almost every new simulation of a natural water body. The remaining steps of the solution consist of only a few matrix multiplications and require a negligible amount of computer time.

The mathematical developments of Chapters 7 and 8 have been rather formidable. In addition, the computer programming required to implement the invariant imbedding solution of the RTE is considerably more complicated than is required for a solution using Monte Carlo methods. However, the computer time required to carry out the calculations shown in Figs. 8.1 and 8.2 is *much less* than the time required to trace the millions (or more) of photon packets required for a Monte Carlo simulation of the full radiance distribution.

The source-free version of the solution algorithm developed here was used to generate the results seen in Mobley (1989) and in Mobley, *et al.* (1993). The results to be seen in Chapter 11 were generated with this same code. The computer code is available from the author; it is documented in Mobley (1988).

choose the quad partitioning scheme, as in Section 4.7

choose the wind speed U

compute the quad-averaged, air-water surface, radiance transfer functions, $t(a,w;r,s{\to}u,v)$, etc., by Monte Carlo ray tracing, as in Section 4.7

compute the spectral amplitudes $\hat{\underline{t}}_p(a,w;k|l)$, etc., from Eqs. (8.49)-(8.51); store results as $\hat{\underline{t}}_p(a,w)$, etc., as in Eq. (8.86)

choose the ith constituent phase function $\tilde{\beta}_i(\mu',\phi'{\to}\mu,\phi)$

compute the quad-averaged phase function $\tilde{\beta}_i(r,s{\to}u,v)$ by Eqs. (8.13) and (8.14)

compute and store the spectral amplitudes $\hat{\beta}^\pm(r,u;l)$ by Eq. (8.34) (repeat these calculations for each constituent phase function, including the phase functions for any inelastic scattering processes)

choose the sky (incident) radiance distribution $L^+(a;\mu,\phi)$

compute the quad-averaged sky radiances $L^+(a;u,v)$ by Eq. (4.52)

compute the amplitudes $\hat{L}_p^+(a;u;l)$ by Eqs. (8.22) and (8.23); store the results as $\underline{\hat{L}}_p^+(a;l)$ by Eq. (8.44a)

(A)

(B)

Ⓐ   Ⓑ

choose the constituent absorption and scattering coefficients, $a_i(\lambda)$ and $b_i(\zeta)$, as in Eqs. (3.10) and (3.11)

choose the true-internal-source path function $L_*^S(\zeta;\mu,\phi)$, as in Eq. (5.107)

compute the quad-averaged, true-internal-source path function $L_*^S(\zeta;u,v)$ by Eq. (8.16)

compute the quad-averaged, inelastic-scattering path function $L_*^I(\zeta;u,v)$, using output from previous runs at other wavelengths, by Eq. (8.15)

compute the effective internal-source amplitudes $\hat{S}_p^\pm(\zeta;u;l)$ by Eqs. (8.22) and (8.23); store the results as $\underline{\hat{S}}_p^\pm(\zeta;l)$ by Eq. (8.44b)

choose the depths $w \equiv \zeta_1 \equiv 0, \zeta_2, ..., \zeta_K \equiv m$, where output is desired

choose the type of bottom boundary to be applied at depth m
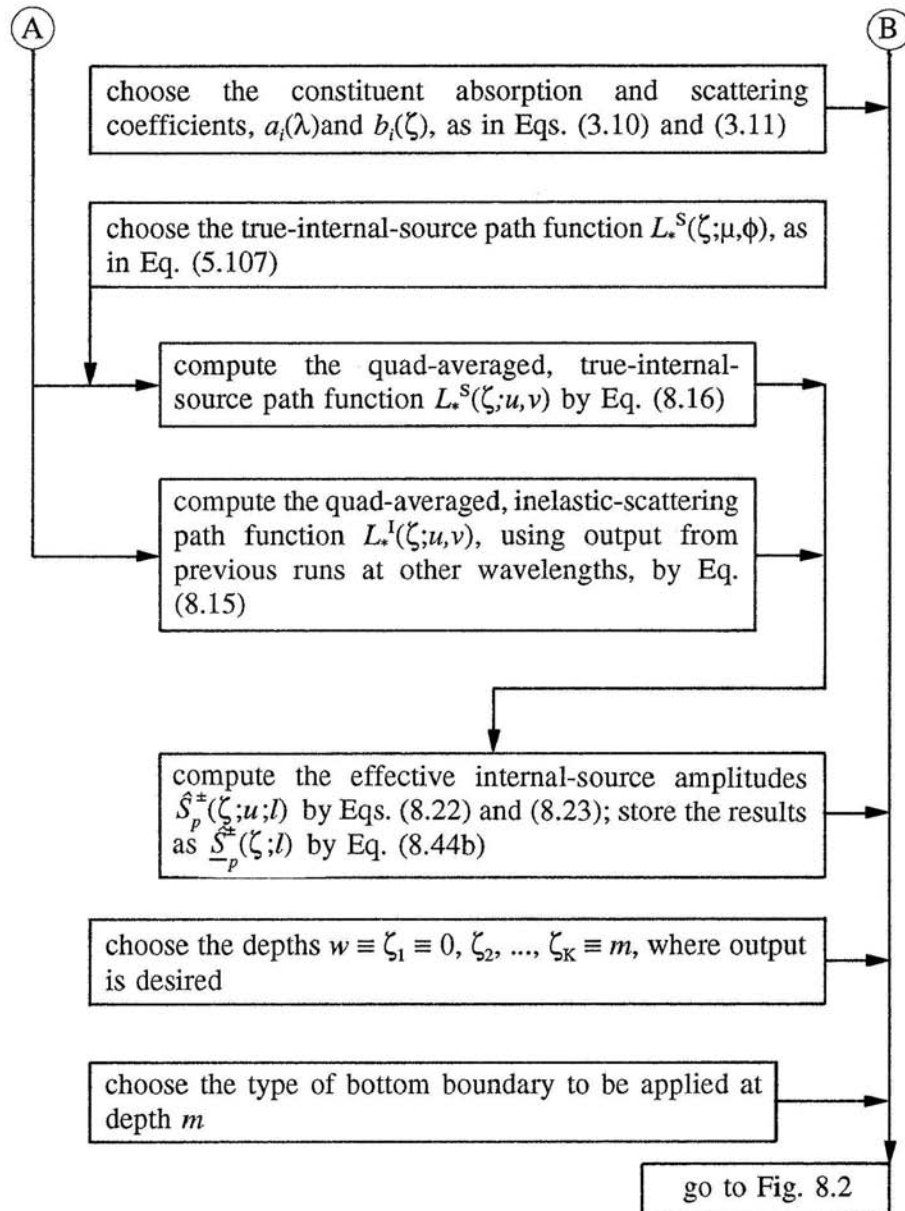
go to Fig. 8.2

Fig. 8.1. Flowchart of the initial calculations required in the invariant imbedding solution of the radiance transfer equation. These calculations define the geometry of the problem; determine the radiance transfer functions for the air-water surface; and define the water inherent optical properties, incident sky radiance, and bottom boundary type.

set $l = 0$

from Fig. 8.1

Obtain $\underline{\rho}(\zeta;l)$ and $\underline{t}(\zeta;l)$ from Eq. (8.42). Integrate the Riccati Eqs. (8.74) and (8.75) in a downward sweep from depth w to depth m, using initial conditions (8.72). Include Eqs. (8.76), (8.78) and (8.79) if internal sources are present.

Compute $\underline{\hat{r}}_p(m,b;l)$ for the chosen type of bottom boundary. Use Eqs. (8.109), (8.55), and (8.57) for a Lambertian bottom, or Eq. (9.76) for an infinitely deep bottom.

Integrate the Riccati Eq. (8.80) in two upward sweeps from m to w, using initial conditions (8.94). Include Eqs. (8.82), (8.84) and (8.85) if internal sources are present.

$l \rightarrow l + 1$

NO

is $l > n$?

YES

Compute $\underline{\hat{L}}_p^+(w)$ using Eq. (8.98)

Compute $\underline{\hat{L}}_p^-(w)$ using Eq. (8.102)

Compute the remaining interior amplitudes $\underline{\hat{L}}_p^\pm(\zeta_k;l)$ using Eqs. (8.105) and (8.106)

Compute $\underline{\hat{L}}_p^-(a)$ using Eq. (8.107)

Compute the quad-averaged radiances $L^\pm(\zeta;u,v)$ using Eq. (8.108)

Compute derived quantities: irradiances, K-functions, reflectances, etc.

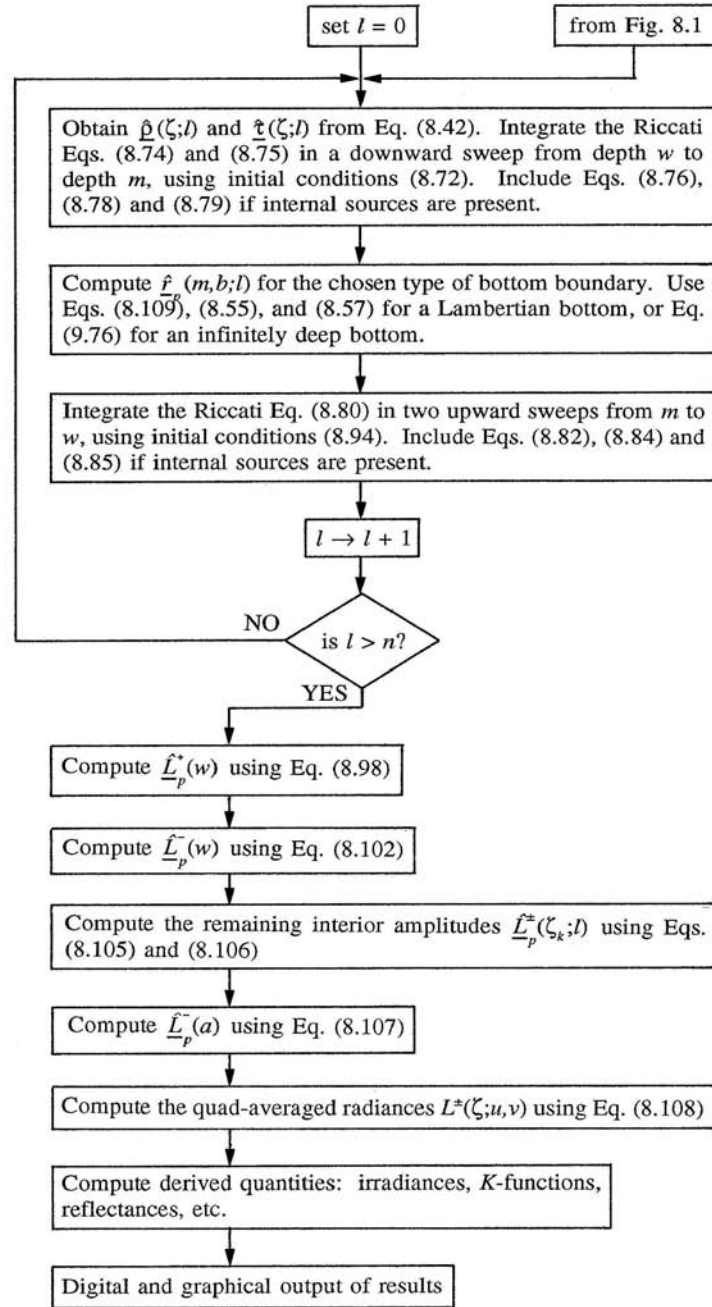Digital and graphical output of results

Fig. 8.2.   Flowchart of the main calculations required in the invariant imbedding solution of the radiance transfer equation. These calculations solve the Riccati equations within the water body, and then incorporate the boundary conditions to obtain the final quad-averaged radiances.

8.11 Problems

8.1. Evaluate $\tilde{\beta}(r,s{\to}u,v)$ for the case of isotropic scattering. What are the units of $\tilde{\beta}(r,s{\to}u,v)$? Now suppose that the unit sphere Ξ is partitioned into two polar caps only; that is, the only "quads" are Ξ_d and Ξ_u. Does your formula for $\tilde{\beta}(r,s{\to}u,v)$ make sense for this special case?

8.2. Consider a surface wave spectrum that has cross-wind, or bi-lateral, symmetry about the wind direction, but which is not symmetric in the upwind-downwind direction. Such a wave spectrum is typical of a well developed sea with all scales of capillary and gravity waves. What simplifications in the air-water surface spectral transfer functions $\hat{t}_{ij}(a,w;r,k|u,l)$, etc., are obtained for such a surface?

8.3. Show by direct calculation using Eqs. (4.63) and (4.81) that the quad-averaged radiance reflectance function for a Lambertian lower boundary is

$$r(m,b;r,s{\to}u,v) \;=\; \frac{R}{\pi}\,\mu_r\,\Omega_{rs}\,.\qquad(8.109)$$

What are the units of $r(m,b;r,s{\to}u,v)$?

8.4. Starting with Eqs. (8.11), (8.31), and (8.54), derive the spectral form of the bottom boundary condition, Eq. (8.56). Be sure to explicitly consider the four cases: (1) quad to quad, (2) quad to polar car, (3) polar cap to quad, and (4) polar cap to polar cap.

8.4. Explicitly evaluate $\hat{i}_1$ for the case of a Lambertian bottom boundary.